Attachment 3 to TMI2-RA-COR-2022-0001

Supplemental Information to License Amendment Request

Three Mile Island Nuclear Station, Unit 2

NRC Possession Only License No. DPR-73

Revision to TMI2-EN-RPT-0002 "MCNP Version 6.2 Bias Determination for Low Enrichment Uranium Using the ENDF/B-VIII.0 Cross Section Library"

ENERGYSOLUTIONS	**Calculation Package**	Doc. No.: TMI2-EN-RPT-0002 Rev.: 1
Title: MCNP Version 6.2 Bias Determination for Low Enrichment Uranium Using the ENDF/B-VIII.0 Cross Section Library		
Design Plan No.: TMI2-DPL-N-00-0001		DP Rev.: 1

Signatures	*(printed name, signature, date)*
Preparer	Derrick Faunce
Approval (Responsible Engineer)	Guy Rhoden

Record of Verification

Item Verified	Acceptable	N/A - Explain
a) Design Verification by Independent Checking Method	☑	☐
b) Computer Software approved per CG-EN-PR-204	☑	☐
c) Calculation Package complete and per CG-EN-PR-203	☑	☐
Signature	*(printed name, signature, date)*	
Verifier	Guy Rhoden	

Record of Revisions

Rev.	Affected Pages	Affected Media	Description	(Print or Type)	
				Preparer	Verifier
0	All	All	Initial Issue	Derrick Faunce	Guy Rhoden
1	4, 12-15	None	Revision to address comments received	Derrick Faunce	Guy Rhoden

Table of Contents

List of Figures

List of Tables

1. INTRODUCTION

1.1. Purpose and Objectives

The following calculation consists of two parts. The first involves the determination of the MCNP Version 6.2 (MCNP6) computer code bias and bias uncertainty. The second part examines the area of applicability (AOA) of the benchmark cases used to determine the bias.

This determination was performed in accordance with ANSI/ANS-8.24-2017, *Validation of Neutron Transport Methods for Nuclear Criticality Safety Calculations* (Ref. [1]). The methodology used in this determination is taken from NUREG/CR-4604, *Statistical Methods for Nuclear Material Management*, (Ref. [2]) and NUREG/CR-6698, *Guide for Validation of Nuclear Criticality Safety Methodology*, (Ref. [3]) which are both listed in Appendix C of ANSI/ANS-8.24.

1.2. Scope

The MCNP6 computer code is validated as appropriate for use in estimating k_{eff} values. This validation report determines the calculational margin and the Margin of Subcriticality (MoS) to establish the maximum Upper Subcritical Limit (USL) for the AOA. Additional margin may be needed for extension of the AOA and is determined in the applicable evaluation, as necessary. The USL is defined as follows:

$$USL = 1 - MoC - MoA - MoS > k_{calc} + 2\sigma_{calc}$$

Where,

MoC is the calculational margin and includes the bias and bias uncertainty (see Section 5.4) in addition to any uncertainties related to trending (see Section 5.3)

MoA is the Margin of Applicability, which is an allowance for any uncertainties related to extenstion of the AOA (see Section 6.2)

MoS is the Margin of Subcriticality, which is an administratve allowance beyond the *MoC* to ensure subcriticality (see Section 6.3)

k_{calc} is the calculated neutron multiplication factor using this validated method

σ_{calc} is the standard deviation associated with k_{calc}

Within this validation report the value *1 – MoC* is collectively referred to as the "*bias*".

The bias determinations were performed based on the use of the ENDF/B-VIII.0 based continuous energy data libraries as prepared by the Los Alamos National Laboratory (LANL). The bias determination was performed for low enrichment uranium (LEU) benchmark models based on the range of process parameters (e.g., enrichment, fissile form) used in this report.

1.3. Hardware and Software Description

The software used herein is Version 6.2 of the MCNP code system. MCNP6 was developed at LANL and acquired from the Radiation Safety Information Computational Center (RSICC). The cross-section library used in this calculation report is the ENDF/B-VIII.0 based library that is processed and distributed by LANL [including thermal scattering S(α,β) libraries]. The specific material libraries used are listed in Section 6.2.

The MCNP6 code system is installed on the NSTS computational platforms NSTS-LS01 and NSTS-LS2. The installation and verification of MCNP6 performance on each NSTS computer is documented in accordance with the Software Qualification and Validation Plan, ESCD-000038, *MCNP6.2 (NSTS) Software Qualification and Validation Plan* (Ref. [4]).

NSTS-LS01 consists of an AMD® Ryzen Threadripper 3970x 32-core processor configured with 32 GB RAM, and the CentOS 8 Linux 64-bit operating system with GNOME desktop environment. NSTS-LS01 is configured for Remote Desktop Access via a secured, encrypted internet connection with enabled firewall.

NSTS-LS2 consists of an AMD® Ryzen Threadripper 3990x 64-core processor configured with 64 GB RAM, and the Fedora 32 Linux 64-bit operating system with the XFCE window manager. NSTS-LS2 is configured to allow authorized access via X2GO software which uses an encrypted secure shell to connect to X2GO client software with the X2GO server on NSTS-LS2.

2. REQUIREMENTS

2.1. Design Inputs

The following present a brief description for each benchmark used. These descriptions are meant only to give the simplest of indication as to the critical configurations represented by the benchmarks. Complete descriptions of the benchmarks can be found in NEA/NSC/DOC(95)03, *International Handbook of Evaluated Criticality Safety Benchmark Experiments*, (Ref. [5]) and should be referred to regarding any detail of the benchmark models discussed herein. A total of 125 benchmark cases are chosen.

2.1.1. LEU-COMP-THERM-002

This benchmark included five configurations that consisted of various arrangements of UO_2 fuel rods. The arrangements are water moderated and reflected.

2.1.2. LEU-COMP-THERM-009

This benchmark included twenty-seven configurations that consisted of various arrangements of UO_2 fuel rods. The fuel rods are arranged in three clusters that are arranged in a single row. Between the clusters are placed plates made of steel, Boral, copper, cadmium, aluminum, or Zircalloy-4. The fuel rods are water moderated and reflected.

2.1.3. LEU-COMP-THERM-013

This benchmark included seven configurations that consisted of three water moderated rectangular cluster of UO_2 fuel rods. The three clusters were separated by plates made of steel, Boral B, Boroflex, cadmium, copper, or copper-cadmium. Two sides of the arrangement of three clusters were reflected by steel walls.

2.1.4. LEU-COMP-THERM-033

This benchmark included fifty-two configurations that consisted rectangular parallelepipeds created from cube blocks of finely divided UF_4 dispersed in paraffin. The configurations were either unreflected or reflected by paraffin or polyethylene.

2.1.5. LEU-COMP-THERM-042

This benchmark included seven configurations that consisted of three water moderated rectangular cluster of UO_2 fuel rods. The three clusters were separated by plates made of steel, Boral B, Boroflex, cadmium, copper, or copper-cadmium. Two sides of the arrangement of three clusters were reflected by steel walls.

2.1.6. LEU-COMP-THERM-049

This benchmark included eighteen configurations that consisted of a stacked array of small boxes filled with UO_2. These were moderated and reflected by polyethylene.

2.1.7. LEU-COMP-THERM-092

This benchmark included six configurations that consisted of an array of stainless-steel-clad cylindrical UO_2 fuel rods. The fuel rods are water moderated and reflected. Control rods consist of Ag-In-Cd. Varying concentrations of soluble boron are in the moderator water.

2.1.8. LEU-SOL-THERM-001

This benchmark included a single configuration that consisted of a cylindrical tank filled with UO_2F_2 solution. The tank was not reflected.

2.1.9. LEU-SOL-THERM-002

This benchmark included three configurations that consisted of spherical geometries of UO_2F_2 solutions with no reflection.

3. REFERENCES

[1] ANSI/ANS-8.24-2017, *Validation of Neutron Transport Methods for Nuclear Criticality Safety Calculations,* American Nuclear Society, 2017.

[2] NUREG/CR-4604, *Statistical Methods for Nuclear Material Management,* Pacific Northwest Laboratory, 1988.

[3] NUREG/CR-6698, *Guide for Validation of Nuclear Criticality Safety Methodology,* Science Applications International Corporation, 2001.

[4] ESCD-000038, Rev. 0, *MCNP6.2 (NSTS) Software Qualification and Validation Plan,* Energy Solutions, 2020.

[5] NEA/NSC/DOC(95)03, *International Handbook of Evaluated Criticality Safety Benchmark Experiments,* National Energy Agency, 2019.

[6] "NIST/SEMATECH e-Handbook of Statistical Methods," October 2013. [Online]. Available: http://www.itl.nist.gov/div898/handbook/.

4. ASSUMPTIONS

None.

5. CALCULATION METHODOLOGY

The following sections present the methods for determination of the bias for MCNP6 based on a selection of experimental benchmarks. The benchmarks represent a selection of uranium based critical experiments that were chosen as being representative of the configurations modeled as part of this report. The description of each experiment may be found in NEA/NSC/DOC(95)03 (Ref. [5]).

For each set of benchmark cases the MCNP6 run parameters were 10,000 neutrons/cycle, 100 skipped cycles, and 5,000 active cycles to minimize the code bias in k_{eff}. All results showed convergence of fission-source entropy (within 1 standard deviation of the average) in less than 40 cycles. Each set of cases were run on the NSTS-LS01 and NSTS-LS2 computers and produced identical results.

5.1. Benchmark Data Preparation

The benchmark data consists of results from MCNP6 calculations and experimental data. Not all the benchmarks resulted in an experimental k_{eff} of exactly 1.0. The benchmarks also have experimental uncertainties that need to be accounted for along with MCNP6 calculation uncertainty. As a result, some preparation of the data must be performed before conducting any statistical analyses.

The first thing that needs to be done is to normalize the k_{eff} values to 1.0 and to combine the MCNP6 and experimental uncertainties. Normalization of the k_{eff} values is needed in those cases where the benchmark experiments have a k_{eff} other than 1.0. This is done using the following formula:

$$k_{adj} = \frac{k_{calc}}{k_{exp}}$$

Where,

k_{adj} = Adjusted calculated k_{eff} value normalized to 1.0

k_{calc} = The MCNP6 calculated k_{eff} value for a benchmark case

k_{exp} = The experimental k_{eff} value for a benchmark case

The combined uncertainty is determined by:

$$\sigma_{com} = \sqrt{{\sigma_{calc}}^2 + {\sigma_{exp}}^2}$$

Where,

σ_{com} = Combined uncertainty

σ_{calc} = The MCNP6 uncertainty for the calculated k_{eff} value for a benchmark case

σ_{exp} = The experimental uncertainty for the k_{eff} value for a benchmark case

5.2. Normality Testing Methodology

5.2.1. Lilliefors Test

The k_{adj} values are examined to determine if they are from a normal distribution. The Lilliefors test as presented in Section 9.6.3.1 of NUREG/CR-4604 (Ref. [2]) was selected given that there are more than 50 values. The first step in this test is to rank the k_{adj} values from smallest to largest and then determine the standardized sample values. As applied to the k_{adj} values, the standardized sample values are determined by the following equation:

$$z_i = \frac{k_i - \bar{k}}{s}$$

Where,

z_i = Standardized sample value for the i^{th} k_{eff} benchmark value

k_i = The k_{adj} value of the i^{th} benchmark case

$\bar{k}$ = The mean of the k_{adj} values

s = Sample standard deviation

The values of z_i are used to determine values of the normal cumulative distribution function (cdf) denoted as F*(z) based on Table A3 in Reference [2]. It is noted that for negative values of z_i, the value of F*(z) is one minus the value from Table A3 in Reference [2] based on the absolute value of z_i. Also note that these values may be readily attained using the 'NORMSDIST()' function in Excel. Next, empirical cumulative distribution function values (denoted as G(z)) are determined for the ordered k_{adj} values. This is simply the ranked value divided by the total number of cases.

The Lilliefors test statistic (T*) is the largest of all values of $|F^*(z_i)-G(z_i)|$ or $|F^*(z_i)-G(z_{i-1})|$. T* is compared to $w_{1-\alpha}$ obtained from Table A18 of Reference [2]. For a 95% confidence level and a sample size over 30, $w_{1-\alpha}$ is given by $\frac{0.886}{\sqrt{n}}$ where n is the number of cases. If T* is less than $w_{1-\alpha}$ the data is probably from a normal distribution.

5.2.2. Normal Probability Plot

The basic description and technique for the normal probability plot are taken from the Section 1.3.3.21 of *NIST/SEMATECH e-Handbook of Statistical Methods* (Ref. [6]). The normal probability plot is formed by:

- Vertical axis: Ordered response values
- Horizontal axis: Normal order statistic medians

The response values are the k_{adj} values ordered from smallest to largest.

The normal order statistic medians are defined by the following function:

$$N_i = G(U_i)$$

Where U_i are the uniform order statistic medians and G is the percent point function of the normal distribution. The percent point function is the inverse of the cumulative distribution function. This provided by the Excel spreadsheet function NORM.S.INV(). The uniform order statistic medians are defined as:

$$U_i = 1 - U_n \text{ for } i=1$$

$$U_i = (i - 0.3175)/(n+0.365) \text{ for } i=2,3,4, \ldots, n-1$$

$$U_i = 0.5^{(1/n)} \text{ for } i=n$$

A straight line is fitted to the data. The further the data departs from the straight line, the greater the indication of departures from normality.

5.3. Trend Analysis Methodology

The benchmark data is examined for potential trends in the k_{adj} data versus the Average Energy of Neutron Energy Causing Fission (AENCF) and also versus the enrichment (wt. % ^{235}U). This is used to determine the proper bias determination method for data that has been determined to come from a normal distribution.

The k_{adj} versus AENCF or enrichment data will be fitted to a number of simple functions along with a determination of the coefficient of determination (R^2). Should the value of R^2 be 0.8 or greater, this would indicate correlation between the data and the fitted function. Depending on the exact nature of the correlated fitted function, a trend in the data that may impact the USL determination is possible. An R^2 value less than 0.8 would indicate either a poor or no correlation between the data and the fitted function.

5.4. Bias Determination Methodology

The methods for determining the bias are presented in this section. Depending on the result of the normality testing one of three methods will be used to determine the bias. The following presents the methods used herein.

5.4.1. Bias Determination for Non-Normal Distributions

For data that is demonstrated to likely *not* come from a normal distribution, the bias is determined based on the nonparametric statistical treatment presented in NUREG/CR-6698 (Ref. [3]). This method results in a determination of the degree of confidence that a fraction of the true population of data lies above the smallest observed value. This is determined with the following equation:

$$\beta = 1 - \sum_{j=0}^{m-1} \frac{n!}{j!\,(n-j)!}(1-q)^j q^{n-j}$$

Where,

q = the desired population fraction (e.g., 0.95)

n = the number of data in one data sample (e.g., number of benchmark cases)

m = the indexed rank from the smallest to the largest.

This equation can be simplified for a desired population fraction of 0.95 and a rank of 1 (smallest data sample) to:

$$\beta = 1 - q^n = 1 - 0.95^n$$

The bias may then be determined by the following:

$$Bias = k_1 - \sigma_1 - NPM$$

Where,

k_1 = Smallest k_{adj} value from the benchmark cases

σ_1 = Standard deviation for smallest k_{adj} value from the benchmark cases

NPM = Nonparametric margin to account for small sample sizes based on the value of β

5.4.2. Bias Determination for Normal Distributions

For data that is demonstrated to likely come from a normal distribution, the bias is determined based one of two methods as described in NUREG/CR-6698 (Ref. [3]). For data that show no trend in k_{adj} versus the AENCF or enrichment the single-sided tolerance limit method is used to determine the bias. For data that show a trend in k_{adj} versus the AENCF or enrichment the one-sided lower tolerance band method is used. For the benchmark data examined herein, the trend information presented in Attachment F – Trend Analysis Figures demonstrates that no trends were present in the data. Therefore, only the single-sided tolerance limit method is presented here.

The bias determined by the single-sided tolerance limit method is defined by the following set equations:

$$Bias = \bar{k}_{adj} - US_p$$

$$U = \frac{z_p + \sqrt{z_p^2 - ab}}{a}$$

$$a = 1 - \frac{z_{1-\alpha}^2}{2(n-1)}$$

$$b = z_p^2 - \frac{z_{1-\alpha}^2}{n}$$

$$\bar{k}_{adj} = \frac{\sum \frac{1}{\sigma_i^2} k_i}{\sum \frac{1}{\sigma_i^2}}$$

$$S_p = \sqrt{s^2 + \bar{\sigma}^2}$$

$$\bar{\sigma}^2 = \frac{1}{\sum \frac{1}{\sigma_i^2}}$$

Where,

$\bar{k}_{adj}$ = Weighted mean k_{adj} value

U = One-sided lower tolerance factor

$z_{1-\alpha}$ = z value for the cumulative standard normal distribution for a confidence value of 1-α

z_p = z value for the cumulative standard normal distribution for a confidence value of p

n = Number of data points (k_{adj} values) in data set

k_i = The i^{th} k_{adj} value

σ_i = Uncertainty of the i^{th} k_{adj} value

S_p = Square root of the pooled variance

$\bar{\sigma}^2$ = Average total variance

6. CALCULATIONS

6.1. Bias Determination

Table 4 in Attachment B – Benchmark Data Set contains the results of the 125 cases used to determine the MCNP6 computer code bias for use with low enrichment ^{235}U fissile materials. Table 4 also contains the experimental result and uncertainty as provided in the benchmark experiments handbook (Ref. [5]), the adjusted k_{eff} (k_{adj}), and combined uncertainty (σ_{com}) for each benchmark. The values for k_{adj} and σ_{com} were determined based on the formulas from Section 5.1. The next step was to order the k_{adj} values from smallest to largest. These ordered values are presented in Attachment C – Tables of k_{adj} Values.

The data was checked to determine if the data come from a normal distribution based on the Lilliefors test discussed in Section 5.2.1. The results of the test are used to help determine which of the bias determination methods from Section 5.4 is used. The Lilliefors test determinations and the bias results are presented in detail in Attachment D – Lilliefors Testing Tables and summarized in Table 1. The normal probability plots are created based on the discussion in Section 5.2.2 as a visual aid. These are shown in Attachment E – Normal Plot Figures.

Table 1. Summary of Lilliefors Test Results and Initial Bias Determination

Observations	$w_{1-\alpha}$	Max T*	Normal Distribution	Bias[1]
125	0.07925	0.19559	No	0.9798
[1] Bias determination details at the bottom of the Lilliefors test table in Attachment D – Lilliefors Testing Tables and includes the bias uncertainty of 0.0006.				

The results of the trend analysis presented in Attachment F – Trend Analysis Figures demonstrate that there is no notable trend within the data that needs to be compensated for in the determination of the bias. The AOA review presented in Section 6.2 should be consulted before using any of the bias results presented in Table 1.

6.2. Area of Applicability Review

The AOA consists of the range or values of various parameters important to the reactivity of the benchmark models. These define the range or values for a system parameter or parameter(s) over which the bias presented above is considered valid without modification. These parameters include such things as fissile material(s), moderators, reflectors, geometry, other significant non-fissile materials (e.g., poisons such as boron or other materials such as steel), and energy characteristics of the experimental system (e.g., fast or thermal). These parameter ranges of the benchmark models are compared to the models of the system being evaluated. If the system parameter ranges fall within the AOA then no additional margin is needed beyond the MoS when determining the USL.

If one or more of the system parameters are found to fall outside of the AOA, then an additional margin of applicability (MoA) may be needed on the USL to extend the applicability of the bias determination. It should be noted that it is anticipated that there will be limited (e.g., one) supporting analyses for TMI-2 decommissioning relying upon this validation report, and that all evaluations are intended to be within this AOA. Nevertheless, the need for an any additional margin based on AOA considerations is addressed in the applicable evaluation, with the following methodology.

If the extension of the system parameter is substantial (e.g., more than 10% outside of the AOA), then this validation report should be revised to include additional critical expermiment benchmarks to enhance the validated AOA. Extension of the AOA to a lesser extent may be made within the analysis with supporting technical justification. This may include sensitivity studies on the effect of changes in the parameter to be extended on k_{eff} of the modeled system, extension of any bias trends noted in this validation report, or other detailed technical justification supporting whether extension of the AOA requires a MoA on the USL.

Table 2. Basic Properties of the MCNP6 Benchmark Models for LEU

Property	LEU AOA					
Fissile Materials	U (2 – 10 wt. % ^{235}U) in the form of compounds (UO_2, UF_4) and solution (UO_2F_2)					
Fissile Geometry	Array of fuel rods, array of rectangular parallelepipeds, cubes in cubic array, finely divided particles in cubes, cylinders, spheres, slabs					
Moderator Materials	Water, Paraffin, Polyethylene					
Reflector Materials	None, Water, Acrylic, Steel, Plexiglas, Paraffin, Polyethylene, Concrete					
Other Significant absorbers, poisons, or structural materials present	Al alloys, steel, borated steel, Boral, boroflex, Ag-In-Cd, Cu, Cu with Cd, Cd, Zircaloy-4, rubber Soluble Boron: 0 – 96 ppm					
Specific Cross Sections and S(α,β) used (MCNP6 identifiers)	1001.00c 5010.00c 5011.00c 6012.00c 6013.00c 7014.00c 8016.00c 8017.00c 9019.00c 11023.00c 12024.00c 12025.00c 12026.00c 13027.00c 14028.00c 14029.00c 14030.00c 15031.00c 16032.00c 16033.00c 16034.00c 16036.00c	17035.00c 17037.00c 19039.00c 19040.00c 19041.00c 20040.00c 20042.00c 20044.00c 20046.00c 20048.00c 22046.00c 22047.00c 22048.00c 22049.00c 22050.00c 24050.00c 24052.00c 24053.00c 24054.00c 25055.00c	26054.00c 26056.00c 26057.00c 26058.00c 27059.00c 28058.00c 28060.00c 28061.00c 28062.00c 28064.00c 29063.00c 29065.00c 30064.00c 30066.00c 30067.00c 30068.00c 30070.00c 40090.00c 40091.00c 40092.00c 40094.00c 40096.00c	42092.00c 42094.00c 42095.00c 42096.00c 42097.00c 42098.00c 42100.00c 47107.00c 47109.00c 48106.00c 48108.00c 48110.00c 48111.00c 48112.00c 48113.00c 48114.00c 48116.00c 49113.00c 49115.00c	50112.00c 50114.00c 50115.00c 50116.00c 50117.00c 50118.00c 50119.00c 50120.00c 50122.00c 50124.00c 92234.00c 92235.00c 92236.00c 92238.00c	h-h2o.40t h-poly.40t
Average Energy of Neutrons Causing Fission	Range (MeV): 2.43E-02 – 2.88E-01 Average (MeV): 1.40E-01					

6.3. Margin of Subcriticality

The MoS is a subcritical margin to ensure that calculational results below the USL are adequately subcritical, and is sometimes referred to as an administrative margin. This value typically ranges from 0.02 (at a minimum) to 0.05, and depends on factors such as the systems to be modeled, the reliability of the calculational method, and knowledge of physical and chemical aspects of the sytems to be modeled. A USL of 0.95 has been typically used for facilities with LEU, and is widely recognized as being adequately subcritical with sufficient subcritical margin. Therefore, assuming a USL of 0.95 (for both normal and credible abnormal conditions), and the bias (including bias uncertainties) of 0.9798, then the implied MoS would be:

$$MoS = USL - Bias = 0.9798 - 0.95 = 0.0298$$

A MoS of 0.0298, that results in a USL of 0.95, is adequate for this AOA as discussed below.

There are a large number of experimental benchmarks utilized in this validation (125 cases covering 9 benchmarks). This provides a large set of cases for the statistical evaluation of the bias and bias uncertainty. Based on the statistical evaluation of the data, the non-parametric (i.e., distribution free) method is used, with sufficient number cases to provide a 95% degree of confidence that 95% of the population lies above the smallest observed value (which requires a minimum of 59 cases). Due to this, there is high confidence that the calculational margin is sufficiently and conservatively quantified for the AOA. The TMI-2 decommissioning operations are for the handling of low enriched uranium (LEU) fuel within a water-moderated system, which is well documented in the benchmark experiments of LEU fuel (as clusters of rods, blocks of UO_2, finely divided UF_4, and solutions of UO_2F_2). These experiments have a high degree of similarity to the anticipated calculations. The anticipated calculations are also simple systems (e.g., spherical, repeating lattice of fuel) with significant conservativisms in the modeling practices such as optimum conditions in moderation, reflection, fuel density, pellet size, and geometry. Additionally, conservative assumptions are made for non-optimized system parameters. For the LEU systems anticipated to be modeled under these conditions, small changes in reactivity (Δk_{eff}) require large changes to the system parameters (e.g., fissile mass). The combination of these factors contribute to the conclusion that there is a high degree of confidence in the calculated k_{eff} values; therefore, a MoS of 0.0298 is determined to be adequate for the resulting USL of 0.95.

7. CONCLUSIONS

This calculation report has determined the bias (including bias uncertainty) for the use of the MCNP Version 6.2 code system and ENDF/B-VIII.0 library installed on the NSTS computers for use in performing calculations that estimate k_{eff} values. The bias values determined herein are applicable to problems that involve low enrichment ^{235}U fissile materials with various moderator and reflector materials. The AOA has been detailed in Section 6.2. The determined bias value is summarized in the following table.

Table 3. Summary of Bias Determination

AOA	Bias
LEU	0.9798

Additionally, this validation report has determined the MoS associated with the anticipated calculations within this AOA to be 0.0298. Therefore, the USL for this AOA is:

$$USL = Bias - MoS - MoA = 0.9798 - 0.0298 - 0 = 0.95$$

Any additional subcritical margin for applications outside the AOA provided in Table 2 (MoA) are to be justified within the applicable evaluation.

Calculations using this method are considered safely subcritical when the following inequality is fulfilled:

$$k_{calc} + 2\sigma_{calc} < USL(0.95)$$

Where,

k_{calc} is the calculated neutron multiplication factor

σ_{calc} is the standard deviation associated with k_{calc}

8. ELECTRONIC FILES

8.1. Computer Runs

Filename	File Date	Computer Code	Ver.	Computer	Filename	File Date	Computer Code	Ver.	Computer
LCT002_01.in	11/12/2020	MCNP	6.2	NSTS-LS01	LCT002_01.in	11/12/2020	MCNP	6.2	NSTS-LS2
LCT002_01.ino	11/18/2020	MCNP	6.2	NSTS-LS01	LCT002_01.ino	11/12/2020	MCNP	6.2	NSTS-LS2
LCT002_02.in	11/12/2020	MCNP	6.2	NSTS-LS01	LCT002_02.in	11/12/2020	MCNP	6.2	NSTS-LS2
LCT002_02.ino	11/18/2020	MCNP	6.2	NSTS-LS01	LCT002_02.ino	11/12/2020	MCNP	6.2	NSTS-LS2
LCT002_03.in	11/12/2020	MCNP	6.2	NSTS-LS01	LCT002_03.in	11/12/2020	MCNP	6.2	NSTS-LS2
LCT002_03.ino	11/18/2020	MCNP	6.2	NSTS-LS01	LCT002_03.ino	11/12/2020	MCNP	6.2	NSTS-LS2
LCT002_04.in	11/12/2020	MCNP	6.2	NSTS-LS01	LCT002_04.in	11/12/2020	MCNP	6.2	NSTS-LS2
LCT002_04.ino	11/18/2020	MCNP	6.2	NSTS-LS01	LCT002_04.ino	11/12/2020	MCNP	6.2	NSTS-LS2
LCT002_05.in	11/12/2020	MCNP	6.2	NSTS-LS01	LCT002_05.in	11/12/2020	MCNP	6.2	NSTS-LS2
LCT002_05.ino	11/18/2020	MCNP	6.2	NSTS-LS01	LCT002_05.ino	11/12/2020	MCNP	6.2	NSTS-LS2
LCT009_01.in	11/12/2020	MCNP	6.2	NSTS-LS01	LCT009_01.in	11/12/2020	MCNP	6.2	NSTS-LS2
LCT009_01.ino	11/18/2020	MCNP	6.2	NSTS-LS01	LCT009_01.ino	11/12/2020	MCNP	6.2	NSTS-LS2
LCT009_02.in	11/12/2020	MCNP	6.2	NSTS-LS01	LCT009_02.in	11/12/2020	MCNP	6.2	NSTS-LS2
LCT009_02.ino	11/18/2020	MCNP	6.2	NSTS-LS01	LCT009_02.ino	11/12/2020	MCNP	6.2	NSTS-LS2
LCT009_03.in	11/12/2020	MCNP	6.2	NSTS-LS01	LCT009_03.in	11/12/2020	MCNP	6.2	NSTS-LS2
LCT009_03.ino	11/18/2020	MCNP	6.2	NSTS-LS01	LCT009_03.ino	11/12/2020	MCNP	6.2	NSTS-LS2
LCT009_04.in	11/12/2020	MCNP	6.2	NSTS-LS01	LCT009_04.in	11/12/2020	MCNP	6.2	NSTS-LS2
LCT009_04.ino	11/18/2020	MCNP	6.2	NSTS-LS01	LCT009_04.ino	11/12/2020	MCNP	6.2	NSTS-LS2
LCT009_05.in	11/12/2020	MCNP	6.2	NSTS-LS01	LCT009_05.in	11/12/2020	MCNP	6.2	NSTS-LS2
LCT009_05.ino	11/18/2020	MCNP	6.2	NSTS-LS01	LCT009_05.ino	11/12/2020	MCNP	6.2	NSTS-LS2
LCT009_06.in	11/12/2020	MCNP	6.2	NSTS-LS01	LCT009_06.in	11/12/2020	MCNP	6.2	NSTS-LS2
LCT009_06.ino	11/18/2020	MCNP	6.2	NSTS-LS01	LCT009_06.ino	11/12/2020	MCNP	6.2	NSTS-LS2
LCT009_07.in	11/12/2020	MCNP	6.2	NSTS-LS01	LCT009_07.in	11/12/2020	MCNP	6.2	NSTS-LS2
LCT009_07.ino	11/18/2020	MCNP	6.2	NSTS-LS01	LCT009_07.ino	11/12/2020	MCNP	6.2	NSTS-LS2
LCT009_08.in	11/12/2020	MCNP	6.2	NSTS-LS01	LCT009_08.in	11/12/2020	MCNP	6.2	NSTS-LS2
LCT009_08.ino	11/18/2020	MCNP	6.2	NSTS-LS01	LCT009_08.ino	11/12/2020	MCNP	6.2	NSTS-LS2
LCT009_09.in	11/12/2020	MCNP	6.2	NSTS-LS01	LCT009_09.in	11/12/2020	MCNP	6.2	NSTS-LS2
LCT009_09.ino	11/18/2020	MCNP	6.2	NSTS-LS01	LCT009_09.ino	11/12/2020	MCNP	6.2	NSTS-LS2
LCT009_10.in	11/12/2020	MCNP	6.2	NSTS-LS01	LCT009_10.in	11/12/2020	MCNP	6.2	NSTS-LS2
LCT009_10.ino	11/18/2020	MCNP	6.2	NSTS-LS01	LCT009_10.ino	11/12/2020	MCNP	6.2	NSTS-LS2
LCT009_11.in	11/12/2020	MCNP	6.2	NSTS-LS01	LCT009_11.in	11/12/2020	MCNP	6.2	NSTS-LS2
LCT009_11.ino	11/18/2020	MCNP	6.2	NSTS-LS01	LCT009_11.ino	11/12/2020	MCNP	6.2	NSTS-LS2
LCT009_12.in	11/12/2020	MCNP	6.2	NSTS-LS01	LCT009_12.in	11/12/2020	MCNP	6.2	NSTS-LS2
LCT009_12.ino	11/18/2020	MCNP	6.2	NSTS-LS01	LCT009_12.ino	11/12/2020	MCNP	6.2	NSTS-LS2
LCT009_13.in	11/12/2020	MCNP	6.2	NSTS-LS01	LCT009_13.in	11/12/2020	MCNP	6.2	NSTS-LS2
LCT009_13.ino	11/18/2020	MCNP	6.2	NSTS-LS01	LCT009_13.ino	11/12/2020	MCNP	6.2	NSTS-LS2
LCT009_14.in	11/12/2020	MCNP	6.2	NSTS-LS01	LCT009_14.in	11/12/2020	MCNP	6.2	NSTS-LS2
LCT009_14.ino	11/18/2020	MCNP	6.2	NSTS-LS01	LCT009_14.ino	11/12/2020	MCNP	6.2	NSTS-LS2
LCT009_15.in	11/12/2020	MCNP	6.2	NSTS-LS01	LCT009_15.in	11/12/2020	MCNP	6.2	NSTS-LS2
LCT009_15.ino	11/18/2020	MCNP	6.2	NSTS-LS01	LCT009_15.ino	11/12/2020	MCNP	6.2	NSTS-LS2

Filename	File Date	Computer Code	Ver.	Computer	Filename	File Date	Computer Code	Ver.	Computer
LCT009_16.in	11/12/2020	MCNP	6.2	NSTS-LS01	LCT009_16.in	11/12/2020	MCNP	6.2	NSTS-LS2
LCT009_16.ino	11/18/2020	MCNP	6.2	NSTS-LS01	LCT009_16.ino	11/12/2020	MCNP	6.2	NSTS-LS2
LCT009_17.in	11/12/2020	MCNP	6.2	NSTS-LS01	LCT009_17.in	11/12/2020	MCNP	6.2	NSTS-LS2
LCT009_17.ino	11/18/2020	MCNP	6.2	NSTS-LS01	LCT009_17.ino	11/12/2020	MCNP	6.2	NSTS-LS2
LCT009_18.in	11/12/2020	MCNP	6.2	NSTS-LS01	LCT009_18.in	11/12/2020	MCNP	6.2	NSTS-LS2
LCT009_18.ino	11/18/2020	MCNP	6.2	NSTS-LS01	LCT009_18.ino	11/12/2020	MCNP	6.2	NSTS-LS2
LCT009_19.in	11/12/2020	MCNP	6.2	NSTS-LS01	LCT009_19.in	11/12/2020	MCNP	6.2	NSTS-LS2
LCT009_19.ino	11/18/2020	MCNP	6.2	NSTS-LS01	LCT009_19.ino	11/12/2020	MCNP	6.2	NSTS-LS2
LCT009_20.in	11/12/2020	MCNP	6.2	NSTS-LS01	LCT009_20.in	11/12/2020	MCNP	6.2	NSTS-LS2
LCT009_20.ino	11/18/2020	MCNP	6.2	NSTS-LS01	LCT009_20.ino	11/12/2020	MCNP	6.2	NSTS-LS2
LCT009_21.in	11/12/2020	MCNP	6.2	NSTS-LS01	LCT009_21.in	11/12/2020	MCNP	6.2	NSTS-LS2
LCT009_21.ino	11/18/2020	MCNP	6.2	NSTS-LS01	LCT009_21.ino	11/12/2020	MCNP	6.2	NSTS-LS2
LCT009_22.in	11/12/2020	MCNP	6.2	NSTS-LS01	LCT009_22.in	11/12/2020	MCNP	6.2	NSTS-LS2
LCT009_22.ino	11/18/2020	MCNP	6.2	NSTS-LS01	LCT009_22.ino	11/12/2020	MCNP	6.2	NSTS-LS2
LCT009_23.in	11/12/2020	MCNP	6.2	NSTS-LS01	LCT009_23.in	11/12/2020	MCNP	6.2	NSTS-LS2
LCT009_23.ino	11/18/2020	MCNP	6.2	NSTS-LS01	LCT009_23.ino	11/12/2020	MCNP	6.2	NSTS-LS2
LCT009_24.in	11/12/2020	MCNP	6.2	NSTS-LS01	LCT009_24.in	11/12/2020	MCNP	6.2	NSTS-LS2
LCT009_24.ino	11/18/2020	MCNP	6.2	NSTS-LS01	LCT009_24.ino	11/12/2020	MCNP	6.2	NSTS-LS2
LCT009_25.in	11/12/2020	MCNP	6.2	NSTS-LS01	LCT009_25.in	11/12/2020	MCNP	6.2	NSTS-LS2
LCT009_25.ino	11/18/2020	MCNP	6.2	NSTS-LS01	LCT009_25.ino	11/12/2020	MCNP	6.2	NSTS-LS2
LCT009_26.in	11/12/2020	MCNP	6.2	NSTS-LS01	LCT009_26.in	11/12/2020	MCNP	6.2	NSTS-LS2
LCT009_26.ino	11/18/2020	MCNP	6.2	NSTS-LS01	LCT009_26.ino	11/12/2020	MCNP	6.2	NSTS-LS2
LCT013_01.in	11/12/2020	MCNP	6.2	NSTS-LS01	LCT013_01.in	11/12/2020	MCNP	6.2	NSTS-LS2
LCT013_01.ino	11/18/2020	MCNP	6.2	NSTS-LS01	LCT013_01.ino	11/12/2020	MCNP	6.2	NSTS-LS2
LCT013_02.in	11/12/2020	MCNP	6.2	NSTS-LS01	LCT013_02.in	11/12/2020	MCNP	6.2	NSTS-LS2
LCT013_02.ino	11/18/2020	MCNP	6.2	NSTS-LS01	LCT013_02.ino	11/12/2020	MCNP	6.2	NSTS-LS2
LCT013_03.in	11/12/2020	MCNP	6.2	NSTS-LS01	LCT013_03.in	11/12/2020	MCNP	6.2	NSTS-LS2
LCT013_03.ino	11/18/2020	MCNP	6.2	NSTS-LS01	LCT013_03.ino	11/12/2020	MCNP	6.2	NSTS-LS2
LCT013_04.in	11/12/2020	MCNP	6.2	NSTS-LS01	LCT013_04.in	11/12/2020	MCNP	6.2	NSTS-LS2
LCT013_04.ino	11/18/2020	MCNP	6.2	NSTS-LS01	LCT013_04.ino	11/12/2020	MCNP	6.2	NSTS-LS2
LCT013_05.in	11/12/2020	MCNP	6.2	NSTS-LS01	LCT013_05.in	11/12/2020	MCNP	6.2	NSTS-LS2
LCT013_05.ino	11/18/2020	MCNP	6.2	NSTS-LS01	LCT013_05.ino	11/12/2020	MCNP	6.2	NSTS-LS2
LCT013_06.in	11/12/2020	MCNP	6.2	NSTS-LS01	LCT013_06.in	11/12/2020	MCNP	6.2	NSTS-LS2
LCT013_06.ino	11/18/2020	MCNP	6.2	NSTS-LS01	LCT013_06.ino	11/12/2020	MCNP	6.2	NSTS-LS2
LCT013_07.in	11/12/2020	MCNP	6.2	NSTS-LS01	LCT013_07.in	11/12/2020	MCNP	6.2	NSTS-LS2
LCT013_07.ino	11/18/2020	MCNP	6.2	NSTS-LS01	LCT013_07.ino	11/12/2020	MCNP	6.2	NSTS-LS2
LCT033_01.in	11/12/2020	MCNP	6.2	NSTS-LS01	LCT033_01.in	11/12/2020	MCNP	6.2	NSTS-LS2
LCT033_01.ino	11/18/2020	MCNP	6.2	NSTS-LS01	LCT033_01.ino	11/12/2020	MCNP	6.2	NSTS-LS2
LCT033_02.in	11/12/2020	MCNP	6.2	NSTS-LS01	LCT033_02.in	11/12/2020	MCNP	6.2	NSTS-LS2
LCT033_02.ino	11/18/2020	MCNP	6.2	NSTS-LS01	LCT033_02.ino	11/12/2020	MCNP	6.2	NSTS-LS2
LCT033_03.in	11/12/2020	MCNP	6.2	NSTS-LS01	LCT033_03.in	11/12/2020	MCNP	6.2	NSTS-LS2
LCT033_03.ino	11/18/2020	MCNP	6.2	NSTS-LS01	LCT033_03.ino	11/12/2020	MCNP	6.2	NSTS-LS2
LCT033_04.in	11/12/2020	MCNP	6.2	NSTS-LS01	LCT033_04.in	11/12/2020	MCNP	6.2	NSTS-LS2
LCT033_04.ino	11/18/2020	MCNP	6.2	NSTS-LS01	LCT033_04.ino	11/12/2020	MCNP	6.2	NSTS-LS2

Filename	File Date	Computer Code	Ver.	Computer	Filename	File Date	Computer Code	Ver.	Computer
LCT033_05.in	11/12/2020	MCNP	6.2	NSTS-LS01	LCT033_05.in	11/12/2020	MCNP	6.2	NSTS-LS2
LCT033_05.ino	11/18/2020	MCNP	6.2	NSTS-LS01	LCT033_05.ino	11/12/2020	MCNP	6.2	NSTS-LS2
LCT033_06.in	11/12/2020	MCNP	6.2	NSTS-LS01	LCT033_06.in	11/12/2020	MCNP	6.2	NSTS-LS2
LCT033_06.ino	11/18/2020	MCNP	6.2	NSTS-LS01	LCT033_06.ino	11/12/2020	MCNP	6.2	NSTS-LS2
LCT033_07.in	11/12/2020	MCNP	6.2	NSTS-LS01	LCT033_07.in	11/12/2020	MCNP	6.2	NSTS-LS2
LCT033_07.ino	11/18/2020	MCNP	6.2	NSTS-LS01	LCT033_07.ino	11/12/2020	MCNP	6.2	NSTS-LS2
LCT033_08.in	11/12/2020	MCNP	6.2	NSTS-LS01	LCT033_08.in	11/12/2020	MCNP	6.2	NSTS-LS2
LCT033_08.ino	11/18/2020	MCNP	6.2	NSTS-LS01	LCT033_08.ino	11/12/2020	MCNP	6.2	NSTS-LS2
LCT033_09.in	11/12/2020	MCNP	6.2	NSTS-LS01	LCT033_09.in	11/12/2020	MCNP	6.2	NSTS-LS2
LCT033_09.ino	11/18/2020	MCNP	6.2	NSTS-LS01	LCT033_09.ino	11/12/2020	MCNP	6.2	NSTS-LS2
LCT033_10.in	11/12/2020	MCNP	6.2	NSTS-LS01	LCT033_10.in	11/12/2020	MCNP	6.2	NSTS-LS2
LCT033_10.ino	11/18/2020	MCNP	6.2	NSTS-LS01	LCT033_10.ino	11/12/2020	MCNP	6.2	NSTS-LS2
LCT033_11.in	11/12/2020	MCNP	6.2	NSTS-LS01	LCT033_11.in	11/12/2020	MCNP	6.2	NSTS-LS2
LCT033_11.ino	11/18/2020	MCNP	6.2	NSTS-LS01	LCT033_11.ino	11/12/2020	MCNP	6.2	NSTS-LS2
LCT033_12.in	11/12/2020	MCNP	6.2	NSTS-LS01	LCT033_12.in	11/12/2020	MCNP	6.2	NSTS-LS2
LCT033_12.ino	11/18/2020	MCNP	6.2	NSTS-LS01	LCT033_12.ino	11/12/2020	MCNP	6.2	NSTS-LS2
LCT033_13.in	11/12/2020	MCNP	6.2	NSTS-LS01	LCT033_13.in	11/12/2020	MCNP	6.2	NSTS-LS2
LCT033_13.ino	11/18/2020	MCNP	6.2	NSTS-LS01	LCT033_13.ino	11/12/2020	MCNP	6.2	NSTS-LS2
LCT033_14.in	11/12/2020	MCNP	6.2	NSTS-LS01	LCT033_14.in	11/12/2020	MCNP	6.2	NSTS-LS2
LCT033_14.ino	11/18/2020	MCNP	6.2	NSTS-LS01	LCT033_14.ino	11/12/2020	MCNP	6.2	NSTS-LS2
LCT033_15.in	11/12/2020	MCNP	6.2	NSTS-LS01	LCT033_15.in	11/12/2020	MCNP	6.2	NSTS-LS2
LCT033_15.ino	11/18/2020	MCNP	6.2	NSTS-LS01	LCT033_15.ino	11/12/2020	MCNP	6.2	NSTS-LS2
LCT033_16.in	11/12/2020	MCNP	6.2	NSTS-LS01	LCT033_16.in	11/12/2020	MCNP	6.2	NSTS-LS2
LCT033_16.ino	11/18/2020	MCNP	6.2	NSTS-LS01	LCT033_16.ino	11/12/2020	MCNP	6.2	NSTS-LS2
LCT033_17.in	11/12/2020	MCNP	6.2	NSTS-LS01	LCT033_17.in	11/12/2020	MCNP	6.2	NSTS-LS2
LCT033_17.ino	11/18/2020	MCNP	6.2	NSTS-LS01	LCT033_17.ino	11/12/2020	MCNP	6.2	NSTS-LS2
LCT033_18.in	11/12/2020	MCNP	6.2	NSTS-LS01	LCT033_18.in	11/12/2020	MCNP	6.2	NSTS-LS2
LCT033_18.ino	11/18/2020	MCNP	6.2	NSTS-LS01	LCT033_18.ino	11/12/2020	MCNP	6.2	NSTS-LS2
LCT033_19.in	11/12/2020	MCNP	6.2	NSTS-LS01	LCT033_19.in	11/12/2020	MCNP	6.2	NSTS-LS2
LCT033_19.ino	11/18/2020	MCNP	6.2	NSTS-LS01	LCT033_19.ino	11/12/2020	MCNP	6.2	NSTS-LS2
LCT033_20.in	11/12/2020	MCNP	6.2	NSTS-LS01	LCT033_20.in	11/12/2020	MCNP	6.2	NSTS-LS2
LCT033_20.ino	11/18/2020	MCNP	6.2	NSTS-LS01	LCT033_20.ino	11/12/2020	MCNP	6.2	NSTS-LS2
LCT033_21.in	11/12/2020	MCNP	6.2	NSTS-LS01	LCT033_21.in	11/12/2020	MCNP	6.2	NSTS-LS2
LCT033_21.ino	11/18/2020	MCNP	6.2	NSTS-LS01	LCT033_21.ino	11/12/2020	MCNP	6.2	NSTS-LS2
LCT033_22.in	11/12/2020	MCNP	6.2	NSTS-LS01	LCT033_22.in	11/12/2020	MCNP	6.2	NSTS-LS2
LCT033_22.ino	11/18/2020	MCNP	6.2	NSTS-LS01	LCT033_22.ino	11/12/2020	MCNP	6.2	NSTS-LS2
LCT033_23.in	11/12/2020	MCNP	6.2	NSTS-LS01	LCT033_23.in	11/12/2020	MCNP	6.2	NSTS-LS2
LCT033_23.ino	11/18/2020	MCNP	6.2	NSTS-LS01	LCT033_23.ino	11/12/2020	MCNP	6.2	NSTS-LS2
LCT033_24.in	11/12/2020	MCNP	6.2	NSTS-LS01	LCT033_24.in	11/12/2020	MCNP	6.2	NSTS-LS2
LCT033_24.ino	11/18/2020	MCNP	6.2	NSTS-LS01	LCT033_24.ino	11/12/2020	MCNP	6.2	NSTS-LS2
LCT033_25.in	11/12/2020	MCNP	6.2	NSTS-LS01	LCT033_25.in	11/12/2020	MCNP	6.2	NSTS-LS2
LCT033_25.ino	11/18/2020	MCNP	6.2	NSTS-LS01	LCT033_25.ino	11/12/2020	MCNP	6.2	NSTS-LS2
LCT033_26.in	11/12/2020	MCNP	6.2	NSTS-LS01	LCT033_26.in	11/12/2020	MCNP	6.2	NSTS-LS2
LCT033_26.ino	11/18/2020	MCNP	6.2	NSTS-LS01	LCT033_26.ino	11/12/2020	MCNP	6.2	NSTS-LS2

Filename	File Date	Computer Code	Ver.	Computer	Filename	File Date	Computer Code	Ver.	Computer
LCT033_27.in	11/12/2020	MCNP	6.2	NSTS-LS01	LCT033_27.in	11/12/2020	MCNP	6.2	NSTS-LS2
LCT033_27.ino	11/18/2020	MCNP	6.2	NSTS-LS01	LCT033_27.ino	11/12/2020	MCNP	6.2	NSTS-LS2
LCT033_28.in	11/12/2020	MCNP	6.2	NSTS-LS01	LCT033_28.in	11/12/2020	MCNP	6.2	NSTS-LS2
LCT033_28.ino	11/18/2020	MCNP	6.2	NSTS-LS01	LCT033_28.ino	11/12/2020	MCNP	6.2	NSTS-LS2
LCT033_29.in	11/12/2020	MCNP	6.2	NSTS-LS01	LCT033_29.in	11/12/2020	MCNP	6.2	NSTS-LS2
LCT033_29.ino	11/18/2020	MCNP	6.2	NSTS-LS01	LCT033_29.ino	11/12/2020	MCNP	6.2	NSTS-LS2
LCT033_30.in	11/12/2020	MCNP	6.2	NSTS-LS01	LCT033_30.in	11/12/2020	MCNP	6.2	NSTS-LS2
LCT033_30.ino	11/18/2020	MCNP	6.2	NSTS-LS01	LCT033_30.ino	11/12/2020	MCNP	6.2	NSTS-LS2
LCT033_31.in	11/12/2020	MCNP	6.2	NSTS-LS01	LCT033_31.in	11/12/2020	MCNP	6.2	NSTS-LS2
LCT033_31.ino	11/18/2020	MCNP	6.2	NSTS-LS01	LCT033_31.ino	11/12/2020	MCNP	6.2	NSTS-LS2
LCT033_32.in	11/12/2020	MCNP	6.2	NSTS-LS01	LCT033_32.in	11/12/2020	MCNP	6.2	NSTS-LS2
LCT033_32.ino	11/18/2020	MCNP	6.2	NSTS-LS01	LCT033_32.ino	11/12/2020	MCNP	6.2	NSTS-LS2
LCT033_33.in	11/12/2020	MCNP	6.2	NSTS-LS01	LCT033_33.in	11/12/2020	MCNP	6.2	NSTS-LS2
LCT033_33.ino	11/18/2020	MCNP	6.2	NSTS-LS01	LCT033_33.ino	11/12/2020	MCNP	6.2	NSTS-LS2
LCT033_34.in	11/12/2020	MCNP	6.2	NSTS-LS01	LCT033_34.in	11/12/2020	MCNP	6.2	NSTS-LS2
LCT033_34.ino	11/18/2020	MCNP	6.2	NSTS-LS01	LCT033_34.ino	11/12/2020	MCNP	6.2	NSTS-LS2
LCT033_35.in	11/12/2020	MCNP	6.2	NSTS-LS01	LCT033_35.in	11/12/2020	MCNP	6.2	NSTS-LS2
LCT033_35.ino	11/18/2020	MCNP	6.2	NSTS-LS01	LCT033_35.ino	11/12/2020	MCNP	6.2	NSTS-LS2
LCT033_36.in	11/12/2020	MCNP	6.2	NSTS-LS01	LCT033_36.in	11/12/2020	MCNP	6.2	NSTS-LS2
LCT033_36.ino	11/18/2020	MCNP	6.2	NSTS-LS01	LCT033_36.ino	11/12/2020	MCNP	6.2	NSTS-LS2
LCT033_37.in	11/12/2020	MCNP	6.2	NSTS-LS01	LCT033_37.in	11/12/2020	MCNP	6.2	NSTS-LS2
LCT033_37.ino	11/18/2020	MCNP	6.2	NSTS-LS01	LCT033_37.ino	11/12/2020	MCNP	6.2	NSTS-LS2
LCT033_38.in	11/12/2020	MCNP	6.2	NSTS-LS01	LCT033_38.in	11/12/2020	MCNP	6.2	NSTS-LS2
LCT033_38.ino	11/18/2020	MCNP	6.2	NSTS-LS01	LCT033_38.ino	11/12/2020	MCNP	6.2	NSTS-LS2
LCT033_39.in	11/12/2020	MCNP	6.2	NSTS-LS01	LCT033_39.in	11/12/2020	MCNP	6.2	NSTS-LS2
LCT033_39.ino	11/18/2020	MCNP	6.2	NSTS-LS01	LCT033_39.ino	11/12/2020	MCNP	6.2	NSTS-LS2
LCT033_40.in	11/12/2020	MCNP	6.2	NSTS-LS01	LCT033_40.in	11/12/2020	MCNP	6.2	NSTS-LS2
LCT033_40.ino	11/18/2020	MCNP	6.2	NSTS-LS01	LCT033_40.ino	11/12/2020	MCNP	6.2	NSTS-LS2
LCT033_41.in	11/12/2020	MCNP	6.2	NSTS-LS01	LCT033_41.in	11/12/2020	MCNP	6.2	NSTS-LS2
LCT033_41.ino	11/18/2020	MCNP	6.2	NSTS-LS01	LCT033_41.ino	11/12/2020	MCNP	6.2	NSTS-LS2
LCT033_42.in	11/12/2020	MCNP	6.2	NSTS-LS01	LCT033_42.in	11/12/2020	MCNP	6.2	NSTS-LS2
LCT033_42.ino	11/18/2020	MCNP	6.2	NSTS-LS01	LCT033_42.ino	11/12/2020	MCNP	6.2	NSTS-LS2
LCT033_43.in	11/12/2020	MCNP	6.2	NSTS-LS01	LCT033_43.in	11/12/2020	MCNP	6.2	NSTS-LS2
LCT033_43.ino	11/18/2020	MCNP	6.2	NSTS-LS01	LCT033_43.ino	11/12/2020	MCNP	6.2	NSTS-LS2
LCT033_44.in	11/12/2020	MCNP	6.2	NSTS-LS01	LCT033_44.in	11/12/2020	MCNP	6.2	NSTS-LS2
LCT033_44.ino	11/18/2020	MCNP	6.2	NSTS-LS01	LCT033_44.ino	11/12/2020	MCNP	6.2	NSTS-LS2
LCT033_45.in	11/12/2020	MCNP	6.2	NSTS-LS01	LCT033_45.in	11/12/2020	MCNP	6.2	NSTS-LS2
LCT033_45.ino	11/18/2020	MCNP	6.2	NSTS-LS01	LCT033_45.ino	11/12/2020	MCNP	6.2	NSTS-LS2
LCT033_46.in	11/12/2020	MCNP	6.2	NSTS-LS01	LCT033_46.in	11/12/2020	MCNP	6.2	NSTS-LS2
LCT033_46.ino	11/18/2020	MCNP	6.2	NSTS-LS01	LCT033_46.ino	11/12/2020	MCNP	6.2	NSTS-LS2
LCT033_47.in	11/12/2020	MCNP	6.2	NSTS-LS01	LCT033_47.in	11/12/2020	MCNP	6.2	NSTS-LS2
LCT033_47.ino	11/18/2020	MCNP	6.2	NSTS-LS01	LCT033_47.ino	11/12/2020	MCNP	6.2	NSTS-LS2
LCT033_48.in	11/12/2020	MCNP	6.2	NSTS-LS01	LCT033_48.in	11/12/2020	MCNP	6.2	NSTS-LS2
LCT033_48.ino	11/18/2020	MCNP	6.2	NSTS-LS01	LCT033_48.ino	11/12/2020	MCNP	6.2	NSTS-LS2

Filename	File Date	Computer Code	Ver.	Computer	Filename	File Date	Computer Code	Ver.	Computer
LCT033_49.in	11/12/2020	MCNP	6.2	NSTS-LS01	LCT033_49.in	11/12/2020	MCNP	6.2	NSTS-LS2
LCT033_49.ino	11/18/2020	MCNP	6.2	NSTS-LS01	LCT033_49.ino	11/12/2020	MCNP	6.2	NSTS-LS2
LCT033_50.in	11/12/2020	MCNP	6.2	NSTS-LS01	LCT033_50.in	11/12/2020	MCNP	6.2	NSTS-LS2
LCT033_50.ino	11/18/2020	MCNP	6.2	NSTS-LS01	LCT033_50.ino	11/12/2020	MCNP	6.2	NSTS-LS2
LCT033_51.in	11/12/2020	MCNP	6.2	NSTS-LS01	LCT033_51.in	11/12/2020	MCNP	6.2	NSTS-LS2
LCT033_51.ino	11/18/2020	MCNP	6.2	NSTS-LS01	LCT033_51.ino	11/12/2020	MCNP	6.2	NSTS-LS2
LCT033_52.in	11/12/2020	MCNP	6.2	NSTS-LS01	LCT033_52.in	11/12/2020	MCNP	6.2	NSTS-LS2
LCT033_52.ino	11/18/2020	MCNP	6.2	NSTS-LS01	LCT033_52.ino	11/12/2020	MCNP	6.2	NSTS-LS2
LCT042_01.in	11/12/2020	MCNP	6.2	NSTS-LS01	LCT042_01.in	11/12/2020	MCNP	6.2	NSTS-LS2
LCT042_01.ino	11/18/2020	MCNP	6.2	NSTS-LS01	LCT042_01.ino	11/12/2020	MCNP	6.2	NSTS-LS2
LCT042_02.in	11/12/2020	MCNP	6.2	NSTS-LS01	LCT042_02.in	11/12/2020	MCNP	6.2	NSTS-LS2
LCT042_02.ino	11/18/2020	MCNP	6.2	NSTS-LS01	LCT042_02.ino	11/12/2020	MCNP	6.2	NSTS-LS2
LCT042_03.in	11/12/2020	MCNP	6.2	NSTS-LS01	LCT042_03.in	11/12/2020	MCNP	6.2	NSTS-LS2
LCT042_03.ino	11/18/2020	MCNP	6.2	NSTS-LS01	LCT042_03.ino	11/12/2020	MCNP	6.2	NSTS-LS2
LCT042_04.in	11/12/2020	MCNP	6.2	NSTS-LS01	LCT042_04.in	11/12/2020	MCNP	6.2	NSTS-LS2
LCT042_04.ino	11/18/2020	MCNP	6.2	NSTS-LS01	LCT042_04.ino	11/12/2020	MCNP	6.2	NSTS-LS2
LCT042_05.in	11/12/2020	MCNP	6.2	NSTS-LS01	LCT042_05.in	11/12/2020	MCNP	6.2	NSTS-LS2
LCT042_05.ino	11/18/2020	MCNP	6.2	NSTS-LS01	LCT042_05.ino	11/12/2020	MCNP	6.2	NSTS-LS2
LCT042_06.in	11/12/2020	MCNP	6.2	NSTS-LS01	LCT042_06.in	11/12/2020	MCNP	6.2	NSTS-LS2
LCT042_06.ino	11/18/2020	MCNP	6.2	NSTS-LS01	LCT042_06.ino	11/12/2020	MCNP	6.2	NSTS-LS2
LCT042_07.in	11/12/2020	MCNP	6.2	NSTS-LS01	LCT042_07.in	11/12/2020	MCNP	6.2	NSTS-LS2
LCT042_07.ino	11/18/2020	MCNP	6.2	NSTS-LS01	LCT042_07.ino	11/12/2020	MCNP	6.2	NSTS-LS2
LCT049_01.in	11/12/2020	MCNP	6.2	NSTS-LS01	LCT049_01.in	11/12/2020	MCNP	6.2	NSTS-LS2
LCT049_01.ino	11/18/2020	MCNP	6.2	NSTS-LS01	LCT049_01.ino	11/12/2020	MCNP	6.2	NSTS-LS2
LCT049_02.in	11/12/2020	MCNP	6.2	NSTS-LS01	LCT049_02.in	11/12/2020	MCNP	6.2	NSTS-LS2
LCT049_02.ino	11/18/2020	MCNP	6.2	NSTS-LS01	LCT049_02.ino	11/12/2020	MCNP	6.2	NSTS-LS2
LCT049_03.in	11/12/2020	MCNP	6.2	NSTS-LS01	LCT049_03.in	11/12/2020	MCNP	6.2	NSTS-LS2
LCT049_03.ino	11/18/2020	MCNP	6.2	NSTS-LS01	LCT049_03.ino	11/12/2020	MCNP	6.2	NSTS-LS2
LCT049_04.in	11/12/2020	MCNP	6.2	NSTS-LS01	LCT049_04.in	11/12/2020	MCNP	6.2	NSTS-LS2
LCT049_04.ino	11/18/2020	MCNP	6.2	NSTS-LS01	LCT049_04.ino	11/12/2020	MCNP	6.2	NSTS-LS2
LCT049_05.in	11/12/2020	MCNP	6.2	NSTS-LS01	LCT049_05.in	11/12/2020	MCNP	6.2	NSTS-LS2
LCT049_05.ino	11/18/2020	MCNP	6.2	NSTS-LS01	LCT049_05.ino	11/12/2020	MCNP	6.2	NSTS-LS2
LCT049_06.in	11/12/2020	MCNP	6.2	NSTS-LS01	LCT049_06.in	11/12/2020	MCNP	6.2	NSTS-LS2
LCT049_06.ino	11/18/2020	MCNP	6.2	NSTS-LS01	LCT049_06.ino	11/12/2020	MCNP	6.2	NSTS-LS2
LCT049_07.in	11/12/2020	MCNP	6.2	NSTS-LS01	LCT049_07.in	11/12/2020	MCNP	6.2	NSTS-LS2
LCT049_07.ino	11/18/2020	MCNP	6.2	NSTS-LS01	LCT049_07.ino	11/12/2020	MCNP	6.2	NSTS-LS2
LCT049_08.in	11/12/2020	MCNP	6.2	NSTS-LS01	LCT049_08.in	11/12/2020	MCNP	6.2	NSTS-LS2
LCT049_08.ino	11/18/2020	MCNP	6.2	NSTS-LS01	LCT049_08.ino	11/12/2020	MCNP	6.2	NSTS-LS2
LCT049_09.in	11/12/2020	MCNP	6.2	NSTS-LS01	LCT049_09.in	11/12/2020	MCNP	6.2	NSTS-LS2
LCT049_09.ino	11/18/2020	MCNP	6.2	NSTS-LS01	LCT049_09.ino	11/12/2020	MCNP	6.2	NSTS-LS2
LCT049_10.in	11/12/2020	MCNP	6.2	NSTS-LS01	LCT049_10.in	11/12/2020	MCNP	6.2	NSTS-LS2
LCT049_10.ino	11/18/2020	MCNP	6.2	NSTS-LS01	LCT049_10.ino	11/12/2020	MCNP	6.2	NSTS-LS2
LCT049_11.in	11/12/2020	MCNP	6.2	NSTS-LS01	LCT049_11.in	11/12/2020	MCNP	6.2	NSTS-LS2
LCT049_11.ino	11/18/2020	MCNP	6.2	NSTS-LS01	LCT049_11.ino	11/12/2020	MCNP	6.2	NSTS-LS2

Filename	File Date	Computer Code	Ver.	Computer	Filename	File Date	Computer Code	Ver.	Computer
LCT049_12.in	11/12/2020	MCNP	6.2	NSTS-LS01	LCT049_12.in	11/12/2020	MCNP	6.2	NSTS-LS2
LCT049_12.ino	11/18/2020	MCNP	6.2	NSTS-LS01	LCT049_12.ino	11/12/2020	MCNP	6.2	NSTS-LS2
LCT049_13.in	11/12/2020	MCNP	6.2	NSTS-LS01	LCT049_13.in	11/12/2020	MCNP	6.2	NSTS-LS2
LCT049_13.ino	11/18/2020	MCNP	6.2	NSTS-LS01	LCT049_13.ino	11/12/2020	MCNP	6.2	NSTS-LS2
LCT049_14.in	11/12/2020	MCNP	6.2	NSTS-LS01	LCT049_14.in	11/12/2020	MCNP	6.2	NSTS-LS2
LCT049_14.ino	11/18/2020	MCNP	6.2	NSTS-LS01	LCT049_14.ino	11/12/2020	MCNP	6.2	NSTS-LS2
LCT049_15.in	11/12/2020	MCNP	6.2	NSTS-LS01	LCT049_15.in	11/12/2020	MCNP	6.2	NSTS-LS2
LCT049_15.ino	11/18/2020	MCNP	6.2	NSTS-LS01	LCT049_15.ino	11/12/2020	MCNP	6.2	NSTS-LS2
LCT049_16.in	11/12/2020	MCNP	6.2	NSTS-LS01	LCT049_16.in	11/12/2020	MCNP	6.2	NSTS-LS2
LCT049_16.ino	11/18/2020	MCNP	6.2	NSTS-LS01	LCT049_16.ino	11/12/2020	MCNP	6.2	NSTS-LS2
LCT049_17.in	11/12/2020	MCNP	6.2	NSTS-LS01	LCT049_17.in	11/12/2020	MCNP	6.2	NSTS-LS2
LCT049_17.ino	11/18/2020	MCNP	6.2	NSTS-LS01	LCT049_17.ino	11/12/2020	MCNP	6.2	NSTS-LS2
LCT049_18.in	11/12/2020	MCNP	6.2	NSTS-LS01	LCT049_18.in	11/12/2020	MCNP	6.2	NSTS-LS2
LCT049_18.ino	11/18/2020	MCNP	6.2	NSTS-LS01	LCT049_18.ino	11/12/2020	MCNP	6.2	NSTS-LS2
LCT092_01.in	11/12/2020	MCNP	6.2	NSTS-LS01	LCT092_01.in	11/12/2020	MCNP	6.2	NSTS-LS2
LCT092_01.ino	11/19/2020	MCNP	6.2	NSTS-LS01	LCT092_01.ino	11/17/2020	MCNP	6.2	NSTS-LS2
LCT092_02.in	11/12/2020	MCNP	6.2	NSTS-LS01	LCT092_02.in	11/12/2020	MCNP	6.2	NSTS-LS2
LCT092_02.ino	11/19/2020	MCNP	6.2	NSTS-LS01	LCT092_02.ino	11/17/2020	MCNP	6.2	NSTS-LS2
LCT092_03.in	11/12/2020	MCNP	6.2	NSTS-LS01	LCT092_03.in	11/12/2020	MCNP	6.2	NSTS-LS2
LCT092_03.ino	11/19/2020	MCNP	6.2	NSTS-LS01	LCT092_03.ino	11/17/2020	MCNP	6.2	NSTS-LS2
LCT092_04.in	11/12/2020	MCNP	6.2	NSTS-LS01	LCT092_04.in	11/12/2020	MCNP	6.2	NSTS-LS2
LCT092_04.ino	11/19/2020	MCNP	6.2	NSTS-LS01	LCT092_04.ino	11/17/2020	MCNP	6.2	NSTS-LS2
LCT092_05.in	11/12/2020	MCNP	6.2	NSTS-LS01	LCT092_05.in	11/12/2020	MCNP	6.2	NSTS-LS2
LCT092_05.ino	11/19/2020	MCNP	6.2	NSTS-LS01	LCT092_05.ino	11/17/2020	MCNP	6.2	NSTS-LS2
LCT092_06.in	11/12/2020	MCNP	6.2	NSTS-LS01	LCT092_06.in	11/12/2020	MCNP	6.2	NSTS-LS2
LCT092_06.ino	11/19/2020	MCNP	6.2	NSTS-LS01	LCT092_06.ino	11/17/2020	MCNP	6.2	NSTS-LS2
LST001_01.in	11/12/2020	MCNP	6.2	NSTS-LS01	LST001_01.in	11/12/2020	MCNP	6.2	NSTS-LS2
LST001_01.ino	11/18/2020	MCNP	6.2	NSTS-LS01	LST001_01.ino	11/12/2020	MCNP	6.2	NSTS-LS2
LST002_01.in	11/12/2020	MCNP	6.2	NSTS-LS01	LST002_01.in	11/12/2020	MCNP	6.2	NSTS-LS2
LST002_01.ino	11/18/2020	MCNP	6.2	NSTS-LS01	LST002_01.ino	11/12/2020	MCNP	6.2	NSTS-LS2
LST002_02.in	11/12/2020	MCNP	6.2	NSTS-LS01	LST002_02.in	11/12/2020	MCNP	6.2	NSTS-LS2
LST002_02.ino	11/18/2020	MCNP	6.2	NSTS-LS01	LST002_02.ino	11/12/2020	MCNP	6.2	NSTS-LS2
LST002_03.in	11/12/2020	MCNP	6.2	NSTS-LS01	LST002_03.in	11/12/2020	MCNP	6.2	NSTS-LS2
LST002_03.ino	11/18/2020	MCNP	6.2	NSTS-LS01	LST002_03.ino	11/12/2020	MCNP	6.2	NSTS-LS2

8.2. Other Electronic Files

Filename	File Date	Description
TMI2-EN-RPT-0002 Data.xlsm	12/10/2020	Data preparation, normality testing, trend analysis, and bias determination

9. ATTACHMENT A – SAMPLE COMPUTER INPUT/OUTPUT

LCT002_01.in

```
M401   10X11 +5 CLUSTER OF U(4.31)O2 RODS, 2.54 CM PITCH
1      1 .069930523  -1 7 -8  u=1 imp:n=1 $ uo2 fuel
2      0   -2 1 7 -8  u=1 imp:n=1 $ gap
3      3 .059751598  -12 2  u=1 imp:n=1 $ clad
4      4 .11734156  -2 8 u=1 imp:n=1 $ rubber end plug (top)
5      4 .11734156  -2 -7 u=1 imp:n=1 $ rubber end plug (bottom)
6      2 .100059  12 u=1 imp:n=1 $ water
7      0  -4 3 -6 5  imp:n=1 lat=1 u=2 fill=1  $ lattice of fuel rods
8      0  -10 11 -20 21 -9 23 fill=2 imp:n=1  $ rod cluster
9      0  -13 11 -21 19 -9 23  imp:n=1 fill=2  $ partial row of fuel rods
10     2 .100059  13 -10 -21 19 -9 23  imp:n=1 $ water of partial row
11     5 .106563  19 -20 11 -10 -23 29  imp:n=1  $ acrylic support plate
12     2 .100059 (-11:10:20:-19:9:-29) -24 25 -26 27 -28 30 imp:n=1 $ water
13     0  24:-25:26:-27:28:-30  imp:n=0

1      c/z 1.27 1.27 .6325  $ fuel cylinder
2      c/z 1.27 1.27 .6415  $ clad inner surface
3      px  0.0  $ fuel rod cell boundary
4      px  2.54  $ fuel rod cell boundary
5      py  0.0  $ fuel rod cell boundary
6      py  2.54  $ fuel rod cell boundary
7      pz  0.0  $ bottom of fuel
8      pz  92.075  $ top of fuel
9      pz  94.2975  $ top of clad
10     px  25.399  $ farthest edge of closest cluster  ***
11     px  .0001  $ closest edge of closest cluster
12     c/z 1.27 1.27 .7075  $ clad outer surface
13     px  12.699   $ edge of partial row  ***
19     py  0.0001  $ close edge of cluster + partial row
20     py  30.479  $ sides of clusters  ***
21     py  2.541  $ side of partial row and full cluster
23     pz  -2.2225  $ bottom of fuel rod
24     px  55.4  $ side of water reflector   ***
25     px  -30  $ side of water reflector
26     py  60.48  $ side of water reflector   ***
27     py  -30  $ side of water reflector
28     pz  107.075  $ top of water
29     pz  -4.7625  $ bottom of acrylic support plate
30     pz  -20.0625  $ bottom of water

kcode 10000 1 100 5100 50000
sdef  x=d1 y=d2 z=d3 cel=d4
si1   0 41
sp1   0 1
si2   0 37
sp2   0 1
si3   0 93
sp3   0 1
si4   l 8
sp4   v
print
c
c     MATERIALS FOR U(4.31)O2 RODS
c
c     m1 is UO2 fuel
m1    92234 5.1835e-6 92235 1.0102e-3
      92236 5.1395e-6 92238 2.2157e-2
      8016  4.6753e-2
c     m2 is water
m2    8016 3.3353e-2  1001 6.6706e-2
mt2   h-h2O.40t
c     m3 is 6061 Al (clad)
m3    13027  5.8433e-2
c Cr Total:    6.2310E-05
       24050     2.7074E-06
```

```
       24052     5.2209E-05
       24053     5.9201E-06
       24054     1.4736E-06
c Cu Total:    6.3731E-05
       29063     4.4083E-05
       29065     1.9648E-05
c Mg Total:    6.6651E-04
       12024     5.2648E-04
       12025     6.6651E-05
       12026     7.3383E-05
c Ti Total:     2.5375E-05
       22046     2.0934E-06
       22047     1.8879E-06
       22048     1.8706E-05
       22049     1.3728E-06
       22050     1.3144E-06
      25055  2.2115e-5
c Si Total:    3.4607E-04
       14028     3.1918E-04
       14029     1.6161E-05
       14030     1.0728E-05
      30064 1.5236E-05
      30066 8.5779E-06
      30067 1.2387E-06
      30068 5.7289E-06
      30070 1.8580E-07
c Fe Total:     1.0152E-04
       26054     5.9338E-06
       26056     9.3149E-05
       26057     2.1512E-06
       26058     2.8629E-07
c     m4 is rubber (end plugs)
m4    6012  4.3083E-02
      6013  4.7918E-04
      1001 5.8178e-2
c Ca Total:    2.5660E-03
       20040     2.4875E-03
       20042     1.6602E-05
       20043     3.4641E-06
       20044     5.3527E-05
       20046     1.0264E-07
       20048     4.7984E-06
       16032 4.7820e-4
c Si Total:    9.6360E-05
       14028     8.8873E-05
       14029     4.5000E-06
       14030     2.9872E-06
        8016  1.2461e-2
mt4   h-poly.40t
c     m5 is acrylic (support plate)
m5    1001 5.6642e-2
      6012  3.5256E-02
      6013  3.9213E-04
      8016 1.4273e-2
mt5   h-poly.40t
```

10. ATTACHMENT B – BENCHMARK DATA SET

The following table provides all the results for all the benchmark cases run. The results are identical for all cases run on NSTS-LS01 and NSTS-LS2.

Table 4: Benchmark Results for MCNP6

Benchmark ID from Ref. [5]	Case #	k_{exp}	σ_{exp}	k_{calc}	σ_{calc}	k_{adj}	σ_{com}
LEU-COMP-THERM-002	1	0.9997	0.0020	0.99854	0.00010	0.9988	0.0020
LEU-COMP-THERM-002	2	0.9997	0.0020	0.99964	0.00010	0.9999	0.0020
LEU-COMP-THERM-002	3	0.9997	0.0020	0.99937	0.00010	0.9997	0.0020
LEU-COMP-THERM-002	4	0.9997	0.0018	0.99884	0.00010	0.9991	0.0018
LEU-COMP-THERM-002	5	0.9997	0.0019	0.99777	0.00010	0.9981	0.0019
LEU-COMP-THERM-009	1	1.0000	0.0021	0.99928	0.00010	0.9993	0.0021
LEU-COMP-THERM-009	2	1.0000	0.0021	0.99890	0.00010	0.9989	0.0021
LEU-COMP-THERM-009	3	1.0000	0.0021	0.99854	0.00010	0.9985	0.0021
LEU-COMP-THERM-009	4	1.0000	0.0021	0.99928	0.00010	0.9993	0.0021
LEU-COMP-THERM-009	5	1.0000	0.0021	0.99962	0.00010	0.9996	0.0021
LEU-COMP-THERM-009	6	1.0000	0.0021	0.99904	0.00010	0.9990	0.0021
LEU-COMP-THERM-009	7	1.0000	0.0021	0.99971	0.00010	0.9997	0.0021
LEU-COMP-THERM-009	8	1.0000	0.0021	0.99884	0.00011	0.9988	0.0021
LEU-COMP-THERM-009	9	1.0000	0.0021	0.99929	0.00011	0.9993	0.0021
LEU-COMP-THERM-009	10	1.0000	0.0021	0.99910	0.00010	0.9991	0.0021
LEU-COMP-THERM-009	11	1.0000	0.0021	0.99916	0.00010	0.9992	0.0021
LEU-COMP-THERM-009	12	1.0000	0.0021	0.99965	0.00010	0.9997	0.0021
LEU-COMP-THERM-009	13	1.0000	0.0021	0.99971	0.00010	0.9997	0.0021
LEU-COMP-THERM-009	14	1.0000	0.0021	0.99786	0.00010	0.9979	0.0021
LEU-COMP-THERM-009	15	1.0000	0.0021	0.99967	0.00010	0.9997	0.0021
LEU-COMP-THERM-009	16	1.0000	0.0021	0.99877	0.00011	0.9988	0.0021
LEU-COMP-THERM-009	17	1.0000	0.0021	0.99971	0.00010	0.9997	0.0021
LEU-COMP-THERM-009	18	1.0000	0.0021	0.99857	0.00010	0.9986	0.0021
LEU-COMP-THERM-009	19	1.0000	0.0021	0.99957	0.00011	0.9996	0.0021
LEU-COMP-THERM-009	20	1.0000	0.0021	0.99886	0.00011	0.9989	0.0021
LEU-COMP-THERM-009	21	1.0000	0.0021	0.99951	0.00010	0.9995	0.0021
LEU-COMP-THERM-009	22	1.0000	0.0021	0.99903	0.00011	0.9990	0.0021
LEU-COMP-THERM-009	23	1.0000	0.0021	0.99971	0.00010	0.9997	0.0021
LEU-COMP-THERM-009	24	1.0000	0.0021	0.99893	0.00010	0.9989	0.0021
LEU-COMP-THERM-009	25	1.0000	0.0021	0.99913	0.00010	0.9991	0.0021
LEU-COMP-THERM-009	26	1.0000	0.0021	0.99938	0.00010	0.9994	0.0021
LEU-COMP-THERM-013	1	1.0000	0.0018	1.00047	0.00011	1.0005	0.0018
LEU-COMP-THERM-013	2	1.0000	0.0018	1.00009	0.00011	1.0001	0.0018
LEU-COMP-THERM-013	3	1.0000	0.0018	0.99992	0.00011	0.9999	0.0018
LEU-COMP-THERM-013	4	1.0000	0.0018	1.00047	0.00011	1.0005	0.0018
LEU-COMP-THERM-013	5	1.0000	0.0032	0.98707	0.00011	0.9871	0.0032
LEU-COMP-THERM-013	6	1.0000	0.0018	0.99967	0.00011	0.9997	0.0018
LEU-COMP-THERM-013	7	1.0000	0.0018	0.99944	0.00011	0.9994	0.0018
LEU-COMP-THERM-033	1	1.0000	0.0038	1.00297	0.00010	1.0030	0.0038
LEU-COMP-THERM-033	2	1.0000	0.0038	1.00360	0.00010	1.0036	0.0038
LEU-COMP-THERM-033	3	1.0000	0.0038	1.00455	0.00010	1.0046	0.0038
LEU-COMP-THERM-033	4	1.0000	0.0038	1.00360	0.00010	1.0036	0.0038

Benchmark ID from Ref. [5]	Case #	k_{exp}	σ_{exp}	k_{calc}	σ_{calc}	k_{adj}	σ_{com}
LEU-COMP-THERM-033	5	1.0000	0.0039	1.00603	0.00010	1.0060	0.0039
LEU-COMP-THERM-033	6	1.0000	0.0039	0.99752	0.00010	0.9975	0.0039
LEU-COMP-THERM-033	7	1.0000	0.0039	0.99756	0.00010	0.9976	0.0039
LEU-COMP-THERM-033	8	1.0000	0.0040	0.99893	0.00010	0.9989	0.0040
LEU-COMP-THERM-033	9	1.0000	0.0040	0.99943	0.00010	0.9994	0.0040
LEU-COMP-THERM-033	10	1.0000	0.0039	0.99141	0.00010	0.9914	0.0039
LEU-COMP-THERM-033	11	1.0000	0.0039	0.99306	0.00009	0.9931	0.0039
LEU-COMP-THERM-033	12	1.0000	0.0039	0.99439	0.00009	0.9944	0.0039
LEU-COMP-THERM-033	13	1.0000	0.0041	1.00164	0.00009	1.0016	0.0041
LEU-COMP-THERM-033	14	1.0000	0.0051	0.99448	0.00007	0.9945	0.0051
LEU-COMP-THERM-033	15	1.0000	0.0051	0.99472	0.00007	0.9947	0.0051
LEU-COMP-THERM-033	16	1.0000	0.0051	0.99499	0.00007	0.9950	0.0051
LEU-COMP-THERM-033	17	1.0000	0.0038	0.99374	0.00011	0.9937	0.0038
LEU-COMP-THERM-033	18	1.0000	0.0038	0.99537	0.00011	0.9954	0.0038
LEU-COMP-THERM-033	19	1.0000	0.0038	0.99765	0.00011	0.9977	0.0038
LEU-COMP-THERM-033	20	1.0000	0.0038	0.99885	0.00011	0.9989	0.0038
LEU-COMP-THERM-033	21	1.0000	0.0038	0.99947	0.00011	0.9995	0.0038
LEU-COMP-THERM-033	22	1.0000	0.0039	1.01380	0.00011	1.0138	0.0039
LEU-COMP-THERM-033	23	1.0000	0.0040	1.00458	0.00011	1.0046	0.0040
LEU-COMP-THERM-033	24	1.0000	0.0040	1.00418	0.00010	1.0042	0.0040
LEU-COMP-THERM-033	25	1.0000	0.0040	1.00342	0.00011	1.0034	0.0040
LEU-COMP-THERM-033	26	1.0000	0.0039	1.00688	0.00010	1.0069	0.0039
LEU-COMP-THERM-033	27	1.0000	0.0039	1.00720	0.00010	1.0072	0.0039
LEU-COMP-THERM-033	28	1.0000	0.0039	1.00735	0.00010	1.0074	0.0039
LEU-COMP-THERM-033	29	1.0000	0.0039	1.00677	0.00011	1.0068	0.0039
LEU-COMP-THERM-033	30	1.0000	0.0039	1.00481	0.00010	1.0048	0.0039
LEU-COMP-THERM-033	31	1.0000	0.0039	1.00436	0.00010	1.0044	0.0039
LEU-COMP-THERM-033	32	1.0000	0.0039	1.00455	0.00010	1.0046	0.0039
LEU-COMP-THERM-033	33	1.0000	0.0039	1.00435	0.00010	1.0044	0.0039
LEU-COMP-THERM-033	34	1.0000	0.0039	1.00446	0.00010	1.0045	0.0039
LEU-COMP-THERM-033	35	1.0000	0.0040	1.00307	0.00010	1.0031	0.0040
LEU-COMP-THERM-033	36	1.0000	0.0040	1.00316	0.00010	1.0032	0.0040
LEU-COMP-THERM-033	37	1.0000	0.0040	1.00254	0.00010	1.0025	0.0040
LEU-COMP-THERM-033	38	1.0000	0.0040	1.00261	0.00010	1.0026	0.0040
LEU-COMP-THERM-033	39	1.0000	0.0040	1.00268	0.00010	1.0027	0.0040
LEU-COMP-THERM-033	40	1.0000	0.0040	1.00219	0.00010	1.0022	0.0040
LEU-COMP-THERM-033	41	1.0000	0.0041	1.00293	0.00009	1.0029	0.0041
LEU-COMP-THERM-033	42	1.0000	0.0041	1.00169	0.00009	1.0017	0.0041
LEU-COMP-THERM-033	43	1.0000	0.0050	1.00079	0.00009	1.0008	0.0050
LEU-COMP-THERM-033	44	1.0000	0.0050	0.99503	0.00007	0.9950	0.0050
LEU-COMP-THERM-033	45	1.0000	0.0050	0.99467	0.00008	0.9947	0.0050
LEU-COMP-THERM-033	46	1.0000	0.0050	0.99409	0.00008	0.9941	0.0050
LEU-COMP-THERM-033	47	1.0000	0.0042	1.01824	0.00012	1.0182	0.0042
LEU-COMP-THERM-033	48	1.0000	0.0042	1.01685	0.00012	1.0169	0.0042
LEU-COMP-THERM-033	49	1.0000	0.0042	1.01700	0.00011	1.0170	0.0042
LEU-COMP-THERM-033	50	1.0000	0.0041	1.01851	0.00012	1.0185	0.0041
LEU-COMP-THERM-033	51	1.0000	0.0041	1.01966	0.00012	1.0197	0.0041
LEU-COMP-THERM-033	52	1.0000	0.0041	1.01572	0.00011	1.0157	0.0041

Benchmark ID from Ref. [5]	Case #	k_{exp}	σ_{exp}	k_{calc}	σ_{calc}	k_{adj}	σ_{com}
LEU-COMP-THERM-042	1	1.0000	0.0016	0.99770	0.00010	0.9977	0.0016
LEU-COMP-THERM-042	2	1.0000	0.0016	0.99756	0.00010	0.9976	0.0016
LEU-COMP-THERM-042	3	1.0000	0.0016	0.99831	0.00010	0.9983	0.0016
LEU-COMP-THERM-042	4	1.0000	0.0017	0.99876	0.00010	0.9988	0.0017
LEU-COMP-THERM-042	5	1.0000	0.0033	0.99871	0.00010	0.9987	0.0033
LEU-COMP-THERM-042	6	1.0000	0.0016	0.99886	0.00010	0.9989	0.0016
LEU-COMP-THERM-042	7	1.0000	0.0018	0.99722	0.00010	0.9972	0.0018
LEU-COMP-THERM-049	1	1.0000	0.0034	0.99564	0.00011	0.9956	0.0034
LEU-COMP-THERM-049	2	1.0000	0.0034	0.99618	0.00011	0.9962	0.0034
LEU-COMP-THERM-049	3	1.0000	0.0034	0.99617	0.00011	0.9962	0.0034
LEU-COMP-THERM-049	4	1.0000	0.0034	0.99655	0.00011	0.9966	0.0034
LEU-COMP-THERM-049	5	1.0000	0.0042	0.99580	0.00011	0.9958	0.0042
LEU-COMP-THERM-049	6	1.0000	0.0042	0.99738	0.00011	0.9974	0.0042
LEU-COMP-THERM-049	7	1.0000	0.0042	0.99650	0.00011	0.9965	0.0042
LEU-COMP-THERM-049	8	1.0000	0.0042	0.99591	0.00011	0.9959	0.0042
LEU-COMP-THERM-049	9	1.0000	0.0037	0.99564	0.00011	0.9956	0.0037
LEU-COMP-THERM-049	10	1.0000	0.0037	0.99784	0.00011	0.9978	0.0037
LEU-COMP-THERM-049	11	1.0000	0.0037	0.99615	0.00011	0.9962	0.0037
LEU-COMP-THERM-049	12	1.0000	0.0037	0.99610	0.00011	0.9961	0.0037
LEU-COMP-THERM-049	13	1.0000	0.0036	0.99562	0.00011	0.9956	0.0036
LEU-COMP-THERM-049	14	1.0000	0.0036	0.99608	0.00011	0.9961	0.0036
LEU-COMP-THERM-049	15	1.0000	0.0036	0.99736	0.00011	0.9974	0.0036
LEU-COMP-THERM-049	16	1.0000	0.0036	0.99667	0.00011	0.9967	0.0036
LEU-COMP-THERM-049	17	1.0000	0.0036	0.99671	0.00011	0.9967	0.0036
LEU-COMP-THERM-049	18	1.0000	0.0030	0.99951	0.00011	0.9995	0.0030
LEU-COMP-THERM-092	1	1.00033	0.00044	1.00089	0.00010	1.0006	0.0005
LEU-COMP-THERM-092	2	1.00033	0.00044	0.99967	0.00010	0.9993	0.0005
LEU-COMP-THERM-092	3	1.00032	0.00044	0.99860	0.00010	0.9983	0.0005
LEU-COMP-THERM-092	4	1.00033	0.00044	0.99632	0.00010	0.9960	0.0005
LEU-COMP-THERM-092	5	1.00033	0.00046	0.99168	0.00010	0.9914	0.0005
LEU-COMP-THERM-092	6	1.00033	0.00055	0.98076	0.00010	0.9804	0.0006
LEU-SOL-THERM-001	1	0.9991	0.0029	1.01215	0.00011	1.0131	0.0029
LEU-SOL-THERM-002	1	1.0038	0.0040	1.00016	0.00008	0.9964	0.0040
LEU-SOL-THERM-002	2	1.0024	0.0037	0.99591	0.00009	0.9935	0.0037
LEU-SOL-THERM-002	3	1.0024	0.0044	1.00101	0.00008	0.9986	0.0044

11. ATTACHMENT C – TABLES OF K_{ADJ} VALUES

The following table contains the ordered k_{adj} values. The MCNP6 output filename is also provided to aid in traceability.

Table 5: Ordered k_{adj} Values for LEU

Filename	Observation	k_{adj}	σ_{com}
LCT092_06.ino	1	0.9804	0.0006
LCT013_05.ino	2	0.9871	0.0032
LCT092_05.ino	3	0.9914	0.0005
LCT033_10.ino	4	0.9914	0.0039
LCT033_11.ino	5	0.9931	0.0039
LST002_02.ino	6	0.9935	0.0037
LCT033_17.ino	7	0.9937	0.0038
LCT033_46.ino	8	0.9941	0.0050
LCT033_12.ino	9	0.9944	0.0039
LCT033_14.ino	10	0.9945	0.0051
LCT033_45.ino	11	0.9947	0.0050
LCT033_15.ino	12	0.9947	0.0051
LCT033_16.ino	13	0.9950	0.0051
LCT033_44.ino	14	0.9950	0.0050
LCT033_18.ino	15	0.9954	0.0038
LCT049_13.ino	16	0.9956	0.0036
LCT049_01.ino	17	0.9956	0.0034
LCT049_09.ino	18	0.9956	0.0037
LCT049_05.ino	19	0.9958	0.0042
LCT049_08.ino	20	0.9959	0.0042
LCT092_04.ino	21	0.9960	0.0005
LCT049_14.ino	22	0.9961	0.0036
LCT049_12.ino	23	0.9961	0.0037
LCT049_11.ino	24	0.9962	0.0037
LCT049_03.ino	25	0.9962	0.0034
LCT049_02.ino	26	0.9962	0.0034
LST002_01.ino	27	0.9964	0.0040
LCT049_07.ino	28	0.9965	0.0042
LCT049_04.ino	29	0.9966	0.0034
LCT049_16.ino	30	0.9967	0.0036
LCT049_17.ino	31	0.9967	0.0036
LCT042_07.ino	32	0.9972	0.0018
LCT049_15.ino	33	0.9974	0.0036
LCT049_06.ino	34	0.9974	0.0042
LCT033_06.ino	35	0.9975	0.0039
LCT033_07.ino	36	0.9976	0.0039
LCT042_02.ino	37	0.9976	0.0016
LCT033_19.ino	38	0.9977	0.0038
LCT042_01.ino	39	0.9977	0.0016
LCT049_10.ino	40	0.9978	0.0037
LCT009_14.ino	41	0.9979	0.0021
LCT002_05.ino	42	0.9981	0.0019
LCT092_03.ino	43	0.9983	0.0005
LCT042_03.ino	44	0.9983	0.0016
LCT009_03.ino	45	0.9985	0.0021

Filename	Observation	k_{adj}	σ_{com}
LCT009_18.ino	46	0.9986	0.0021
LST002_03.ino	47	0.9986	0.0044
LCT042_05.ino	48	0.9987	0.0033
LCT042_04.ino	49	0.9988	0.0017
LCT009_16.ino	50	0.9988	0.0021
LCT002_01.ino	51	0.9988	0.0020
LCT009_08.ino	52	0.9988	0.0021
LCT033_20.ino	53	0.9989	0.0038
LCT009_20.ino	54	0.9989	0.0021
LCT042_06.ino	55	0.9989	0.0016
LCT009_02.ino	56	0.9989	0.0021
LCT009_24.ino	57	0.9989	0.0021
LCT033_08.ino	58	0.9989	0.0040
LCT009_22.ino	59	0.9990	0.0021
LCT009_06.ino	60	0.9990	0.0021
LCT009_10.ino	61	0.9991	0.0021
LCT009_25.ino	62	0.9991	0.0021
LCT002_04.ino	63	0.9991	0.0018
LCT009_11.ino	64	0.9992	0.0021
LCT009_01.ino	65	0.9993	0.0021
LCT009_04.ino	66	0.9993	0.0021
LCT009_09.ino	67	0.9993	0.0021
LCT092_02.ino	68	0.9993	0.0005
LCT009_26.ino	69	0.9994	0.0021
LCT033_09.ino	70	0.9994	0.0040
LCT013_07.ino	71	0.9994	0.0018
LCT033_21.ino	72	0.9995	0.0038
LCT009_21.ino	73	0.9995	0.0021
LCT049_18.ino	74	0.9995	0.0030
LCT009_19.ino	75	0.9996	0.0021
LCT009_05.ino	76	0.9996	0.0021
LCT009_12.ino	77	0.9997	0.0021
LCT002_03.ino	78	0.9997	0.0020
LCT009_15.ino	79	0.9997	0.0021
LCT013_06.ino	80	0.9997	0.0018
LCT009_07.ino	81	0.9997	0.0021
LCT009_13.ino	82	0.9997	0.0021
LCT009_17.ino	83	0.9997	0.0021
LCT009_23.ino	84	0.9997	0.0021
LCT013_03.ino	85	0.9999	0.0018
LCT002_02.ino	86	0.9999	0.0020
LCT013_02.ino	87	1.0001	0.0018
LCT013_01.ino	88	1.0005	0.0018
LCT013_04.ino	89	1.0005	0.0018
LCT092_01.ino	90	1.0006	0.0005
LCT033_43.ino	91	1.0008	0.0050
LCT033_13.ino	92	1.0016	0.0041
LCT033_42.ino	93	1.0017	0.0041
LCT033_40.ino	94	1.0022	0.0040
LCT033_37.ino	95	1.0025	0.0040
LCT033_38.ino	96	1.0026	0.0040
LCT033_39.ino	97	1.0027	0.0040

Filename	Observation	k_{adj}	σ_{com}
LCT033_41.ino	98	1.0029	0.0041
LCT033_01.ino	99	1.0030	0.0038
LCT033_35.ino	100	1.0031	0.0040
LCT033_36.ino	101	1.0032	0.0040
LCT033_25.ino	102	1.0034	0.0040
LCT033_02.ino	103	1.0036	0.0038
LCT033_04.ino	104	1.0036	0.0038
LCT033_24.ino	105	1.0042	0.0040
LCT033_33.ino	106	1.0044	0.0039
LCT033_31.ino	107	1.0044	0.0039
LCT033_34.ino	108	1.0045	0.0039
LCT033_03.ino	109	1.0046	0.0038
LCT033_32.ino	110	1.0046	0.0039
LCT033_23.ino	111	1.0046	0.0040
LCT033_30.ino	112	1.0048	0.0039
LCT033_05.ino	113	1.0060	0.0039
LCT033_29.ino	114	1.0068	0.0039
LCT033_26.ino	115	1.0069	0.0039
LCT033_27.ino	116	1.0072	0.0039
LCT033_28.ino	117	1.0074	0.0039
LST001_01.ino	118	1.0131	0.0029
LCT033_22.ino	119	1.0138	0.0039
LCT033_52.ino	120	1.0157	0.0041
LCT033_48.ino	121	1.0169	0.0042
LCT033_49.ino	122	1.0170	0.0042
LCT033_47.ino	123	1.0182	0.0042
LCT033_50.ino	124	1.0185	0.0041
LCT033_51.ino	125	1.0197	0.0041

12. ATTACHMENT D – LILLIEFORS TESTING TABLES

Table 6: Lilliefors Normality Test Determination for MCNP6 Benchmark Results for LEU

Case #	k_{adj}	σ_{com}	z_i	F(z)	G(z)	$\lvert F^*(z_i)-G(z_i)\rvert$	$\lvert F^*(z_i)-G(z_{i-1})\rvert$
1	0.9804	0.0006	-3.40840	0.00033	0.00800	0.00767	0.00033
2	0.9871	0.0032	-2.25560	0.01205	0.01600	0.00395	0.00405
3	0.9914	0.0005	-1.51131	0.06535	0.02400	0.04135	0.04935
4	0.9914	0.0039	-1.50138	0.06663	0.03200	0.03463	0.04263
5	0.9931	0.0039	-1.21464	0.11225	0.04000	0.07225	0.08025
6	0.9935	0.0037	-1.13374	0.12845	0.04800	0.08045	0.08845
7	0.9937	0.0038	-1.09647	0.13644	0.05600	0.08044	0.08844
8	0.9941	0.0050	-1.03564	0.15018	0.06400	0.08618	0.09418
9	0.9944	0.0039	-0.98351	0.16268	0.07200	0.09068	0.09868
10	0.9945	0.0051	-0.96787	0.16656	0.08000	0.08656	0.09456
11	0.9947	0.0050	-0.93485	0.17493	0.08800	0.08693	0.09493
12	0.9947	0.0051	-0.92616	0.17718	0.09600	0.08118	0.08918
13	0.9950	0.0051	-0.87924	0.18964	0.10400	0.08564	0.09364
14	0.9950	0.0050	-0.87229	0.19153	0.11200	0.07953	0.08753
15	0.9954	0.0038	-0.81320	0.20805	0.12000	0.08805	0.09605
16	0.9956	0.0036	-0.76975	0.22072	0.12800	0.09272	0.10072
17	0.9956	0.0034	-0.76628	0.22176	0.13600	0.08576	0.09376
18	0.9956	0.0037	-0.76628	0.22176	0.14400	0.07776	0.08576
19	0.9958	0.0042	-0.73847	0.23011	0.15200	0.07811	0.08611
20	0.9959	0.0042	-0.71936	0.23596	0.16000	0.07596	0.08396
21	0.9960	0.0005	-0.70522	0.24034	0.16800	0.07234	0.08034
22	0.9961	0.0036	-0.68981	0.24516	0.17600	0.06916	0.07716
23	0.9961	0.0037	-0.68634	0.24625	0.18400	0.06225	0.07025
24	0.9962	0.0037	-0.67765	0.24900	0.19200	0.05700	0.06500
25	0.9962	0.0034	-0.67417	0.25010	0.20000	0.05010	0.05810
26	0.9962	0.0034	-0.67244	0.25065	0.20800	0.04265	0.05065
27	0.9964	0.0040	-0.63876	0.26149	0.21600	0.04549	0.05349
28	0.9965	0.0042	-0.61682	0.26868	0.22400	0.04468	0.05268
29	0.9966	0.0034	-0.60814	0.27155	0.23200	0.03955	0.04755
30	0.9967	0.0036	-0.58728	0.27851	0.24000	0.03851	0.04651
31	0.9967	0.0036	-0.58033	0.28085	0.24800	0.03285	0.04085
32	0.9972	0.0018	-0.49170	0.31147	0.25600	0.05547	0.06347
33	0.9974	0.0036	-0.46737	0.32012	0.26400	0.05612	0.06412
34	0.9974	0.0042	-0.46390	0.32136	0.27200	0.04936	0.05736
35	0.9975	0.0039	-0.43957	0.33013	0.28000	0.05013	0.05813
36	0.9976	0.0039	-0.43261	0.33265	0.28800	0.04465	0.05265
37	0.9976	0.0016	-0.43261	0.33265	0.29600	0.03665	0.04465
38	0.9977	0.0038	-0.41697	0.33835	0.30400	0.03435	0.04235
39	0.9977	0.0016	-0.40829	0.34153	0.31200	0.02953	0.03753
40	0.9978	0.0037	-0.38396	0.35051	0.32000	0.03051	0.03851
41	0.9979	0.0021	-0.38048	0.35179	0.32800	0.02379	0.03179
42	0.9981	0.0019	-0.34409	0.36539	0.33600	0.02939	0.03739
43	0.9983	0.0005	-0.30740	0.37927	0.34400	0.03527	0.04327
44	0.9983	0.0016	-0.30228	0.38122	0.35200	0.02922	0.03722
45	0.9985	0.0021	-0.26231	0.39654	0.36000	0.03654	0.04454
46	0.9986	0.0021	-0.25709	0.39855	0.36800	0.03055	0.03855
47	0.9986	0.0044	-0.24956	0.40146	0.37600	0.02546	0.03346
48	0.9987	0.0033	-0.23276	0.40797	0.38400	0.02397	0.03197

Case #	k_{adj}	σ_{com}	z_i	F(z)	G(z)	$\lvert F^*(z_i)-G(z_i)\rvert$	$\lvert F^*(z_i)-G(z_{i-1})\rvert$
49	0.9988	0.0017	-0.22407	0.41135	0.39200	0.01935	0.02735
50	0.9988	0.0021	-0.22234	0.41203	0.40000	0.01203	0.02003
51	0.9988	0.0020	-0.21023	0.41674	0.40800	0.00874	0.01674
52	0.9988	0.0021	-0.21017	0.41677	0.41600	0.00077	0.00877
53	0.9989	0.0038	-0.20843	0.41744	0.42400	0.00656	0.00144
54	0.9989	0.0021	-0.20670	0.41812	0.43200	0.01388	0.00588
55	0.9989	0.0016	-0.20670	0.41812	0.44000	0.02188	0.01388
56	0.9989	0.0021	-0.19975	0.42084	0.44800	0.02716	0.01916
57	0.9989	0.0021	-0.19453	0.42288	0.45600	0.03312	0.02512
58	0.9989	0.0040	-0.19453	0.42288	0.46400	0.04112	0.03312
59	0.9990	0.0021	-0.17715	0.42969	0.47200	0.04231	0.03431
60	0.9990	0.0021	-0.17542	0.43038	0.48000	0.04962	0.04162
61	0.9991	0.0021	-0.16499	0.43448	0.48800	0.05352	0.04552
62	0.9991	0.0021	-0.15978	0.43653	0.49600	0.05947	0.05147
63	0.9991	0.0018	-0.15808	0.43720	0.50400	0.06680	0.05880
64	0.9992	0.0021	-0.15456	0.43858	0.51200	0.07342	0.06542
65	0.9993	0.0021	-0.13371	0.44682	0.52000	0.07318	0.06518
66	0.9993	0.0021	-0.13371	0.44682	0.52800	0.08118	0.07318
67	0.9993	0.0021	-0.13197	0.44750	0.53600	0.08850	0.08050
68	0.9993	0.0005	-0.12324	0.45096	0.54400	0.09304	0.08504
69	0.9994	0.0021	-0.11633	0.45370	0.55200	0.09830	0.09030
70	0.9994	0.0040	-0.10764	0.45714	0.56000	0.10286	0.09486
71	0.9994	0.0018	-0.10590	0.45783	0.56800	0.11017	0.10217
72	0.9995	0.0038	-0.10069	0.45990	0.57600	0.11610	0.10810
73	0.9995	0.0021	-0.09374	0.46266	0.58400	0.12134	0.11334
74	0.9995	0.0030	-0.09374	0.46266	0.59200	0.12934	0.12134
75	0.9996	0.0021	-0.08331	0.46680	0.60000	0.13320	0.12520
76	0.9996	0.0021	-0.07462	0.47026	0.60800	0.13774	0.12974
77	0.9997	0.0021	-0.06941	0.47233	0.61600	0.14367	0.13567
78	0.9997	0.0020	-0.06595	0.47371	0.62400	0.15029	0.14229
79	0.9997	0.0021	-0.06593	0.47372	0.63200	0.15828	0.15028
80	0.9997	0.0018	-0.06593	0.47372	0.64000	0.16628	0.15828
81	0.9997	0.0021	-0.05898	0.47648	0.64800	0.17152	0.16352
82	0.9997	0.0021	-0.05898	0.47648	0.65600	0.17952	0.17152
83	0.9997	0.0021	-0.05898	0.47648	0.66400	0.18752	0.17952
84	0.9997	0.0021	-0.05898	0.47648	0.67200	0.19552	0.18752
85	0.9999	0.0018	-0.02249	0.49103	0.68000	0.18897	0.18097
86	0.9999	0.0020	-0.01901	0.49241	0.68800	0.19559	0.18759
87	1.0001	0.0018	0.00706	0.50282	0.69600	0.19318	0.18518
88	1.0005	0.0018	0.07309	0.52913	0.70400	0.17487	0.16687
89	1.0005	0.0018	0.07309	0.52913	0.71200	0.18287	0.17487
90	1.0006	0.0005	0.08870	0.53534	0.72000	0.18466	0.17666
91	1.0008	0.0050	0.12870	0.55120	0.72800	0.17680	0.16880
92	1.0016	0.0041	0.27642	0.60889	0.73600	0.12711	0.11911
93	1.0017	0.0041	0.28511	0.61222	0.74400	0.13178	0.12378
94	1.0022	0.0040	0.37200	0.64505	0.75200	0.10695	0.09895
95	1.0025	0.0040	0.43283	0.66743	0.76000	0.09257	0.08457
96	1.0026	0.0040	0.44499	0.67184	0.76800	0.09616	0.08816
97	1.0027	0.0040	0.45715	0.67622	0.77600	0.09978	0.09178
98	1.0029	0.0041	0.50060	0.69167	0.78400	0.09233	0.08433
99	1.0030	0.0038	0.50755	0.69412	0.79200	0.09788	0.08988
100	1.0031	0.0040	0.52493	0.70018	0.80000	0.09982	0.09182

Case #	k_{adj}	σ_{com}	z_i	F(z)	G(z)	$\lvert F^*(z_i)-G(z_i)\rvert$	$\lvert F^*(z_i)-G(z_{i-1})\rvert$
101	1.0032	0.0040	0.54057	0.70560	0.80800	0.10240	0.09440
102	1.0034	0.0040	0.58575	0.72098	0.81600	0.09502	0.08702
103	1.0036	0.0038	0.61704	0.73139	0.82400	0.09261	0.08461
104	1.0036	0.0038	0.61704	0.73139	0.83200	0.10061	0.09261
105	1.0042	0.0040	0.71783	0.76357	0.84000	0.07643	0.06843
106	1.0044	0.0039	0.74737	0.77258	0.84800	0.07542	0.06742
107	1.0044	0.0039	0.74911	0.77310	0.85600	0.08290	0.07490
108	1.0045	0.0039	0.76649	0.77831	0.86400	0.08569	0.07769
109	1.0046	0.0038	0.78213	0.78293	0.87200	0.08907	0.08107
110	1.0046	0.0039	0.78213	0.78293	0.88000	0.09707	0.08907
111	1.0046	0.0040	0.78734	0.78446	0.88800	0.10354	0.09554
112	1.0048	0.0039	0.82731	0.79597	0.89600	0.10003	0.09203
113	1.0060	0.0039	1.03933	0.85067	0.90400	0.05333	0.04533
114	1.0068	0.0039	1.16793	0.87858	0.91200	0.03342	0.02542
115	1.0069	0.0039	1.18704	0.88239	0.92000	0.03761	0.02961
116	1.0072	0.0039	1.24265	0.89300	0.92800	0.03500	0.02700
117	1.0074	0.0039	1.26872	0.89773	0.93600	0.03827	0.03027
118	1.0131	0.0029	2.26133	0.98813	0.94400	0.04413	0.05213
119	1.0138	0.0039	2.38962	0.99157	0.95200	0.03957	0.04757
120	1.0157	0.0041	2.72329	0.99677	0.96000	0.03677	0.04477
121	1.0169	0.0042	2.91966	0.99825	0.96800	0.03025	0.03825
122	1.0170	0.0042	2.94573	0.99839	0.97600	0.02239	0.03039
123	1.0182	0.0042	3.16122	0.99921	0.98400	0.01521	0.02321
124	1.0185	0.0041	3.20814	0.99933	0.99200	0.00733	0.01533
125	1.0197	0.0041	3.40799	0.99967	1.00000	0.00033	0.00767

Lilliefors Test Results

$\bar{k}$ = 1.0000	s = 0.0058	n=125	$w_{1-\alpha}$=0.07925	Max T*=0.19559

T* > $w_{1-\alpha}$ therefore these cases are probably *not* from a normal distribution. As such the nonparametric method is used to define the bias as described in Section 5.4.1.	k_1=0.9804; σ_1=0.0006 β = 99.99%; NPM (125) = 0 (Table 2.2, NUREG/CR-6698, Ref. [3]) Bias = 0.9804 – 0.0006 Bias = 0.9798

13. ATTACHMENT E – NORMAL PLOT FIGURES

The following figure is the normal probability plot of results identified in Section 6.1.

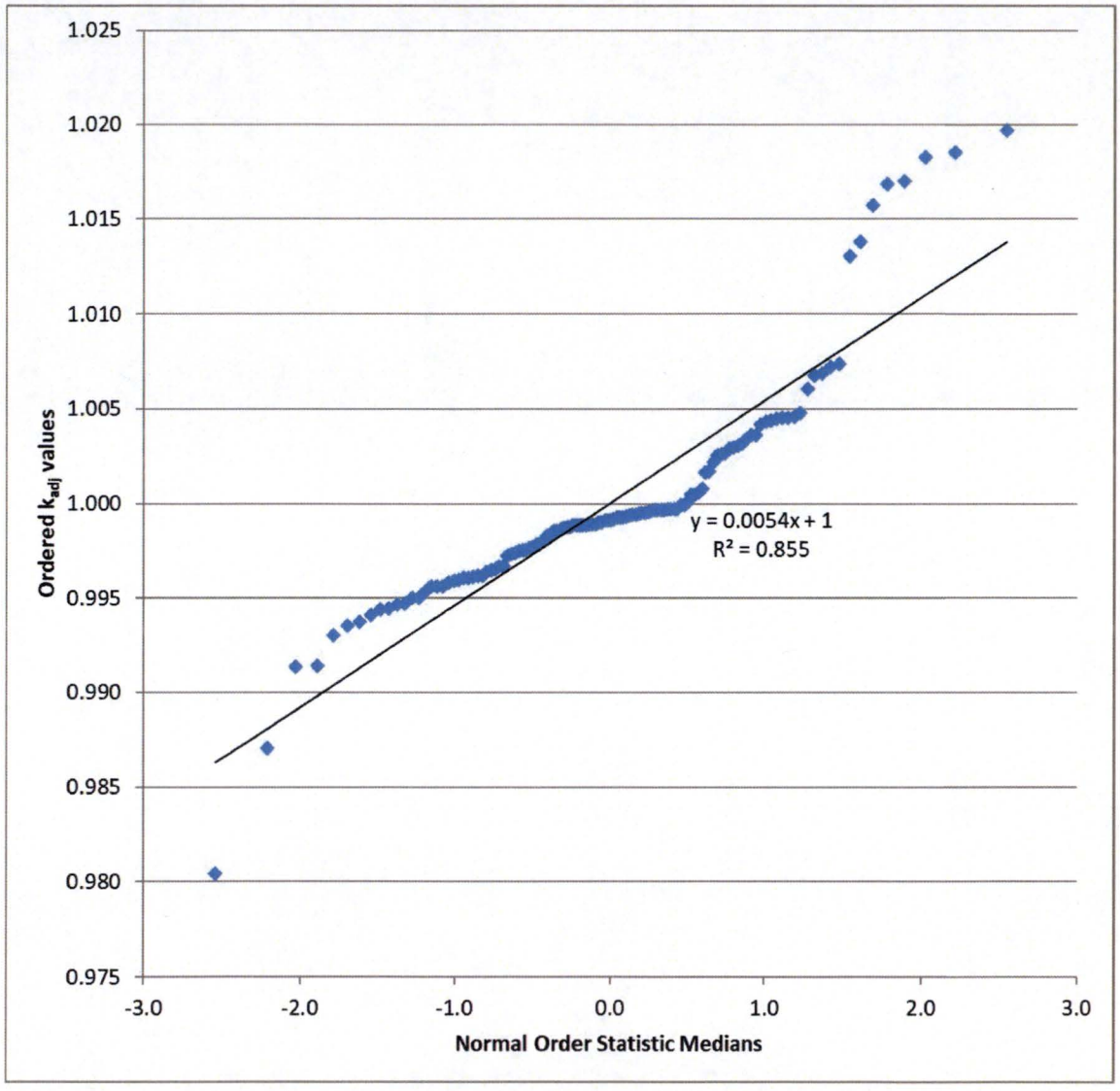

Figure 1: Normal Probability Plot for LEU k_{adj} Results

14. ATTACHMENT F – TREND ANALYSIS FIGURES

The following figures present the results of the trend analysis performed on the k_{adj} values over the range of ANECF and enrichment. The data is fitted to a linear, a 3rd order polynomial, and a power function. The best fit of these functions is shown in the figures along with the determined value of R^2.

The largest R^2 value was 0.2 for the k_{adj} vs. enrichment data fitted to a 3rd order polynomial. None of the data resulted in a R^2 value greater than 0.8 which indicates that none of the data demonstrated a good correlation with the various assumed functions. Therefore, none of the data is considered to demonstrate any significant or relevant trend that would need to be compensated for in the bias.

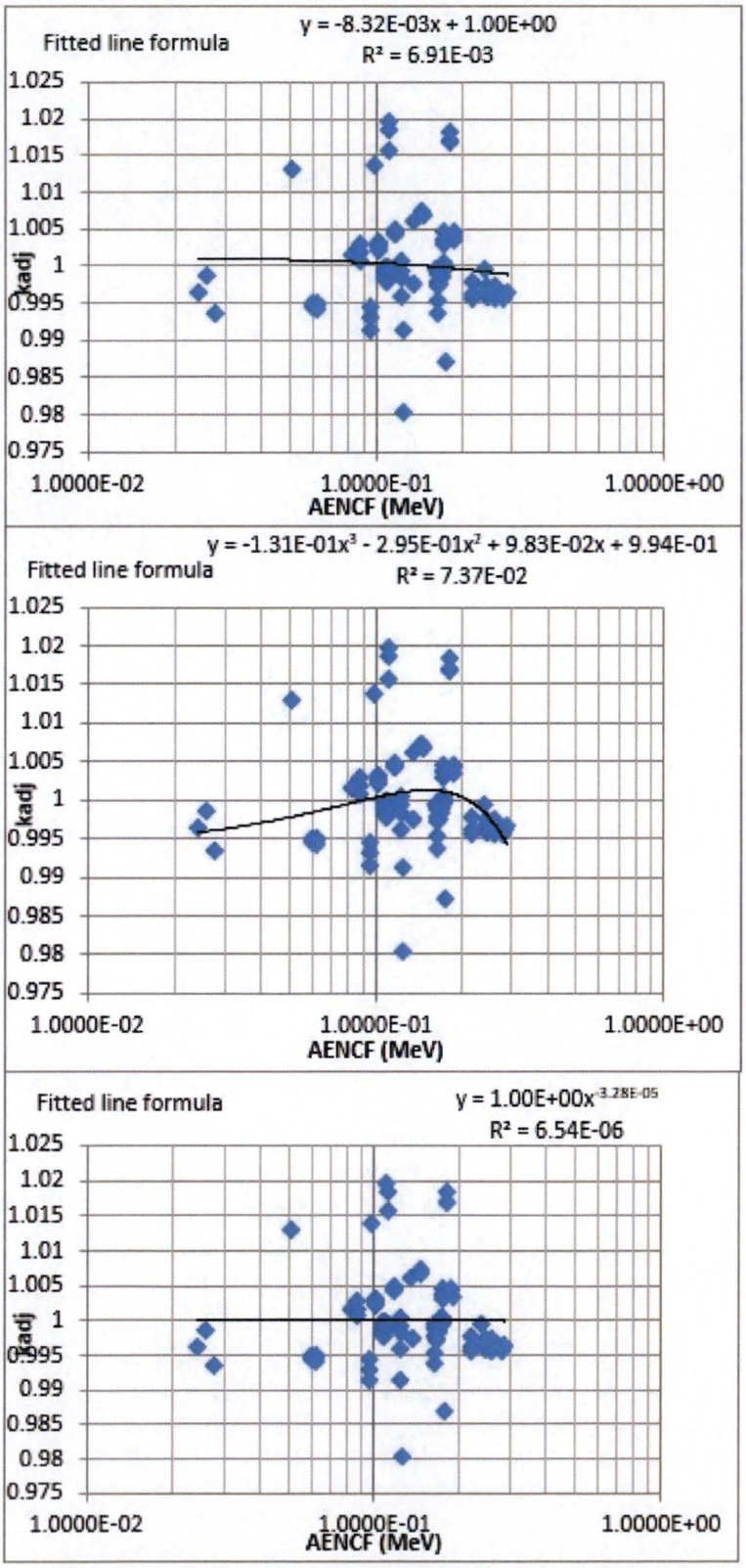

Figure 2: ANECF Trend Analysis Plots for LEU

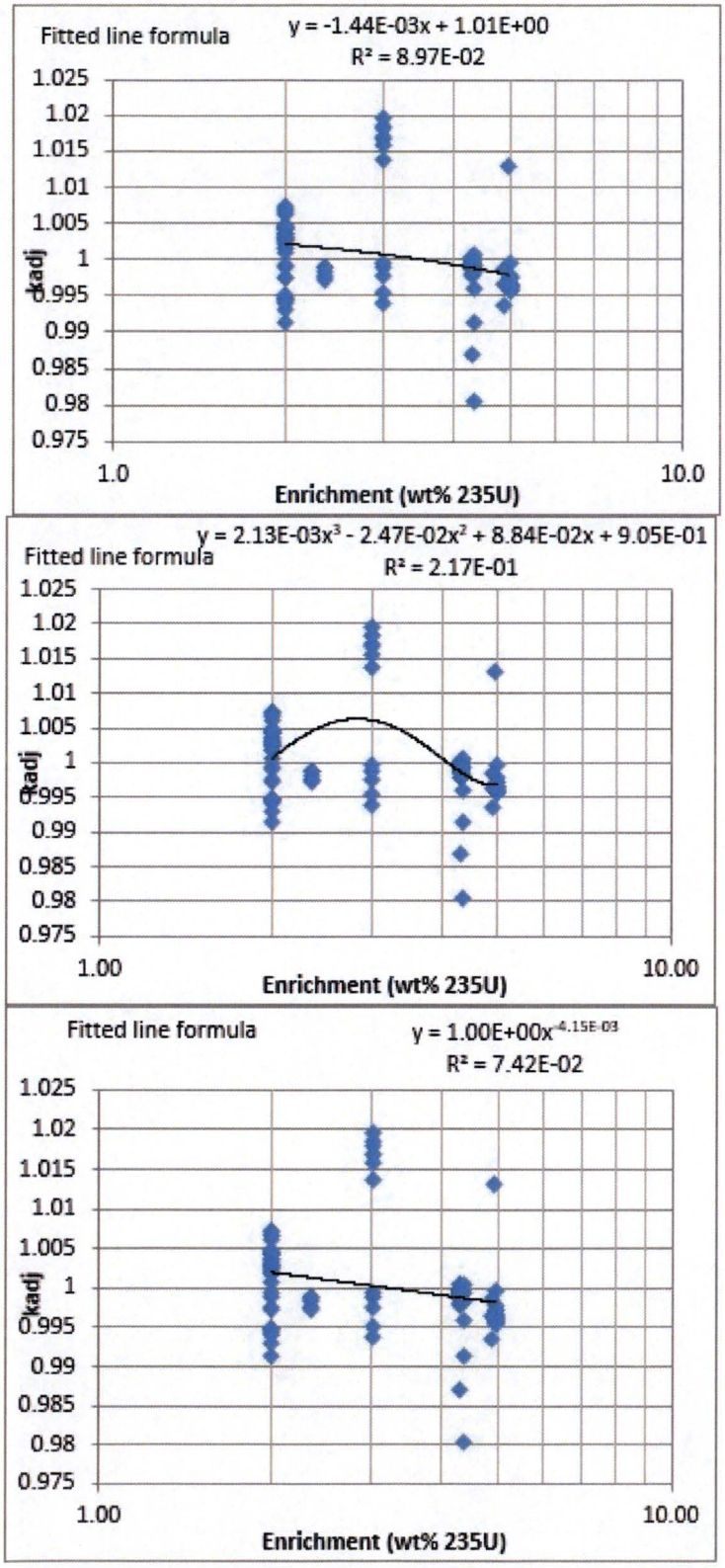

Figure 3: Enrichment Trend Analysis Plots for LEU